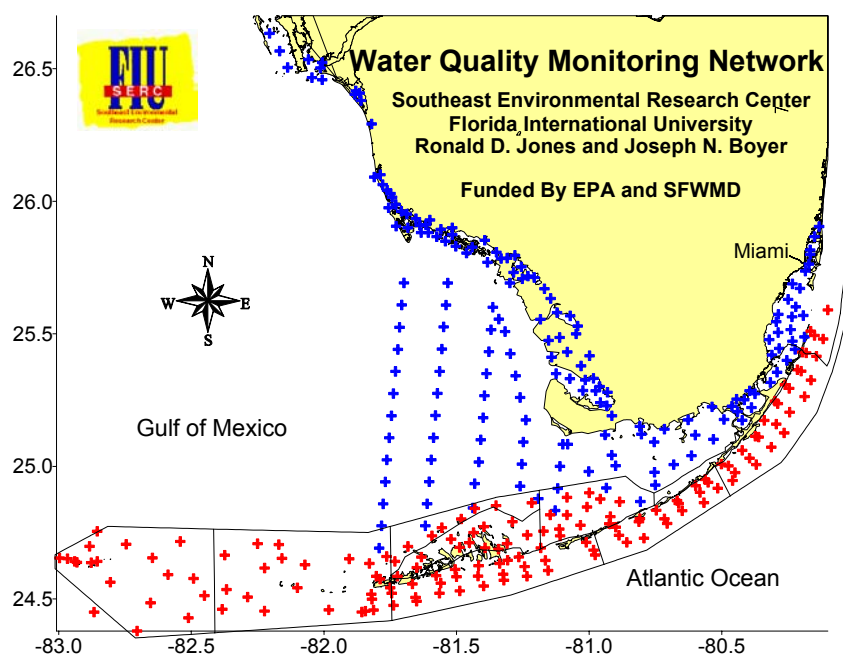


# FY2002 ANNUAL REPORT OF THE WATER QUALITY MONITORING PROJECT

## FOR THE WATER QUALITY PROTECTION PROGRAM

### IN THE FLORIDA KEYS NATIONAL MARINE SANCTUARY



Southeast Environmental Research Center  
Florida International University  
Miami, FL 33199

<http://serc.fiu.edu/wqmnetwork/>

**FY2002 ANNUAL REPORT OF THE WATER  
QUALITY MONITORING PROJECT**

**FOR THE WATER QUALITY PROTECTION PROGRAM**

**IN THE FLORIDA KEYS NATIONAL MARINE SANCTUARY**

Principal Investigators

Ronald D. Jones

and

Joseph N. Boyer

Southeast Environmental Research Center  
Florida International University  
Miami, FL 33199  
<http://serc.fiu.edu/wqmnetwork/>

US EPA Contract #X994621-94-0  
SFWMD/SERC Agreement C-13178  
Monroe County Tourist Development Council

This is Technical Report #T192 of the Southeast Environmental Research Center  
at Florida International University.

**FY2002 ANNUAL REPORT OF THE WATER QUALITY MONITORING PROJECT  
FOR THE WATER QUALITY PROTECTION PROGRAM  
IN THE FLORIDA KEYS NATIONAL MARINE SANCTUARY**

Funded by the Environmental Protection Agency (X994621-94-0), South Florida Water Management District (#C-13178), and Monroe County Tourist Development Council

Ronald D. Jones and Joseph N. Boyer, Southeast Environmental Research Center,  
Florida International University, Miami, FL 33199

**EXECUTIVE SUMMARY**

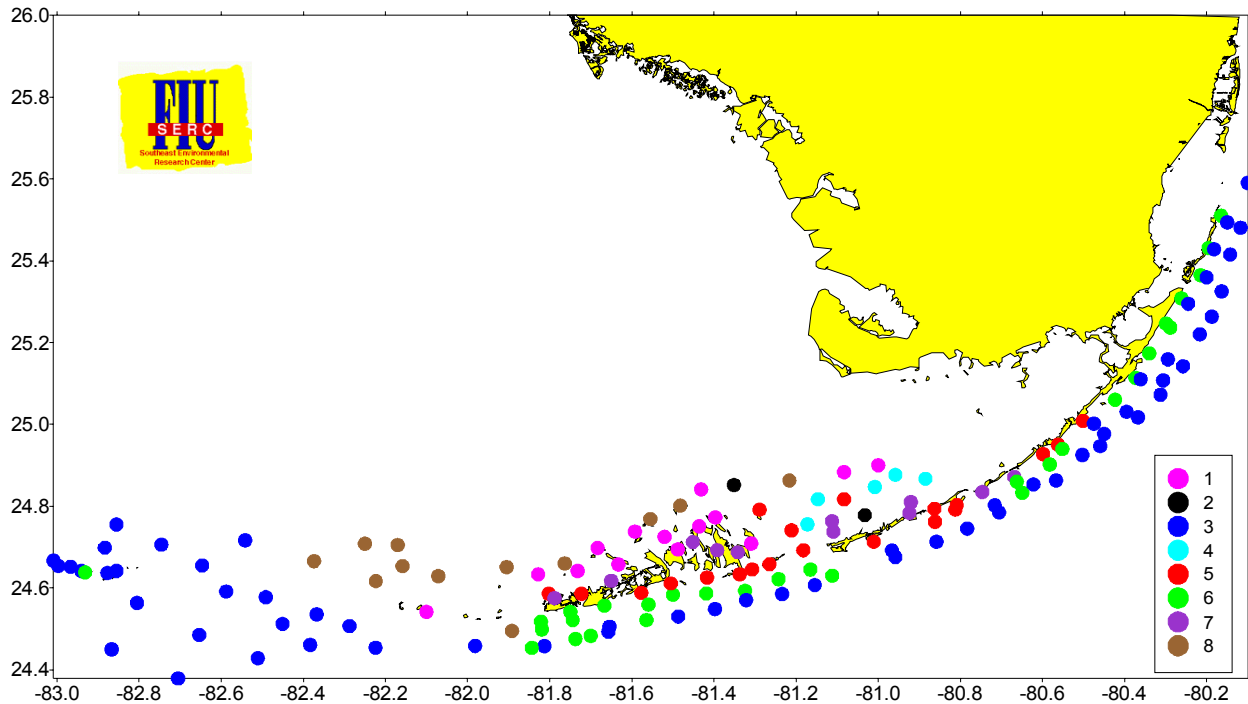
This report serves as a summary of our efforts to date in the execution of the Water Quality Monitoring Project for the FKNMS as part of the Water Quality Protection Program. The period of record for this report is Mar. 1995 – Sept. 2002 and includes data from 29 quarterly sampling events at 154 stations within the FKNMS including the Dry Tortugas National Park.

Field parameters at each station include salinity (practical salinity scale), temperature (°C), dissolved oxygen (DO, mg l<sup>-1</sup>), turbidity (NTU), relative fluorescence, and light attenuation (K<sub>d</sub>, m<sup>-1</sup>). Water chemistry variables include the dissolved nutrients nitrate (NO<sub>3</sub><sup>-</sup>), nitrite (NO<sub>2</sub><sup>-</sup>), ammonium (NH<sub>4</sub><sup>+</sup>), dissolved inorganic nitrogen (DIN), and soluble reactive phosphate (SRP). Total unfiltered concentrations of nitrogen (TN), organic nitrogen (TON), organic carbon (TOC), phosphorus (TP), and silicate (Si(OH)<sub>4</sub>) were also measured. Biological parameters included chlorophyll *a* (CHLA, µg l<sup>-1</sup>) and alkaline phosphatase activity (APA, µM h<sup>-1</sup>). All concentrations are reported as µM unless noted otherwise.

On a vertical basis, temperature, DO, TOC, and TON were generally higher in surface waters while salinity, NO<sub>3</sub><sup>-</sup>, NO<sub>2</sub><sup>-</sup>, NH<sub>4</sub><sup>+</sup>, TP, and turbidity were higher in bottom waters. This slight stratification is indicative of a weak pycnocline which is maintained by freshwater inputs, advection of lower salinity waters from Florida Bay and the SW Shelf, and solar heating at the surface. Elevated nutrient concentrations in bottom waters are due to benthic flux and episodic upwelling from deep offshore waters.

An Objective Classification Analysis was performed in an effort to group stations in the FKNMS according to their specific water quality. This resulted in the formation of 8 clusters of stations which possessed distinct signatures in water quality. We believe this is a more functional zonation of the FKNMS, for our analyses, as it is not biased by subjective delineations but by similarities in the physical, chemical, and biological attributes of the water masses. The bulk of the stations fell into 6 large clusters which described a gradient of water quality

throughout the FKNMS. Although the differences among them were subtle, they were statistically significant and allowed us to report that the overall nutrient gradient, from highest to lowest concentrations, was cluster 7&8>1>5>6>3.



Cluster 7 (●) was highest in inorganic nutrients, especially  $\text{NO}_3^-$ , as well as TOC and TON. Cluster 8 (●) had the highest CHLA and turbidity while being low in inorganic and organic nutrients and as such was driven by water quality of the Shelf. Cluster 1 (●) was high in TP, CHLA, and turbidity. The main distinction between Cluster 1 and 8 was higher in CHLA and lower in TOC. Cluster 5 (●) was elevated in DIN relative to the Hawk Channel and reef tract sites. Cluster 6 (●) was slightly lower in nutrients than Cluster 5. Cluster 3 (●) had the lowest nutrients, CHLA, turbidity, and TOC of any in the FKNMS. A clear gradient of elevated DIN, TP, TOC, and turbidity from alongshore to offshore was observed in the Keys with the Upper Keys being lower than the Middle and Lower Keys. No gradient was observed for CHLA.

Temporal trends in water quality showed most variables to be relatively consistent from year to year, with some showing seasonal excursions. The exception was the increasing variability in TP concentrations throughout the region. This brings up an important point that, when looking at what are perceived to be local trends, we find that they seem to occur across the whole region but at more damped amplitudes. This spatial autocorrelation in water quality is an inherent property of highly interconnected systems such as coastal and estuarine ecosystems driven by

similar hydrological and climatological forcings. Clearly, there have been large changes in the FKNMS water quality over time, but no sustained monotonic trends have been observed. We must always keep in mind that trend analysis is limited to the window of observation; trends may change with additional data collection.

The large scale of this monitoring program has allowed us to assemble a much more holistic view of broad physical/chemical/biological interactions occurring over the South Florida hydroscape. Much information has been gained by inference from this type of data collection program: major nutrient sources have been confirmed, relative differences in geographical determinants of water quality have been demonstrated, and large scale transport via circulation pathways have been elucidated. In addition we have shown the importance of looking "outside the box" for questions asked within. Rather than thinking of water quality monitoring as being a static, non-scientific pursuit it should be viewed as a tool for answering management questions and developing new scientific hypotheses.

We continue to maintain a website (<http://serc.fiu.edu/wqmnetwork/>) where data from the FKNMS is integrated with the other parts of the SERC water quality network (Florida Bay, Whitewater Bay, Biscayne Bay, Ten Thousand Islands, and SW Florida Shelf) and displayed as downloadable contour maps, time series graphs, and interpretive reports.

# **Table of Contents**

**I. PROJECT BACKGROUND**

**II. METHODS**

**III. RESULTS**

**IV. DISCUSSION**

**V. REFERENCES**

**VI. APPENDIX – CONTOUR MAPS**

## I. Project Background

The Florida Keys are a archipelago of sub-tropical islands of Pleistocene origin which extend in a NE to SW direction from Miami to Key West and out to the Dry Tortugas (Fig. 1). In 1990, President Bush signed into law the Florida Keys National Sanctuary and Protection Act (HR5909) which designated a boundary encompassing >2,800 square nautical miles of islands, coastal waters, and coral reef tract as the Florida Keys National Marine Sanctuary (FKNMS). The Comprehensive Management Plan (NOAA 1995) required the FKNMS to have a Water Quality Protection Plan (WQPP) thereafter developed by EPA and the State of Florida (EPA 1995). The contract for the water quality monitoring component of the WQPP was subsequently awarded to the Southeast Environmental Research Program at Florida International University and the field sampling program began in March 1995.

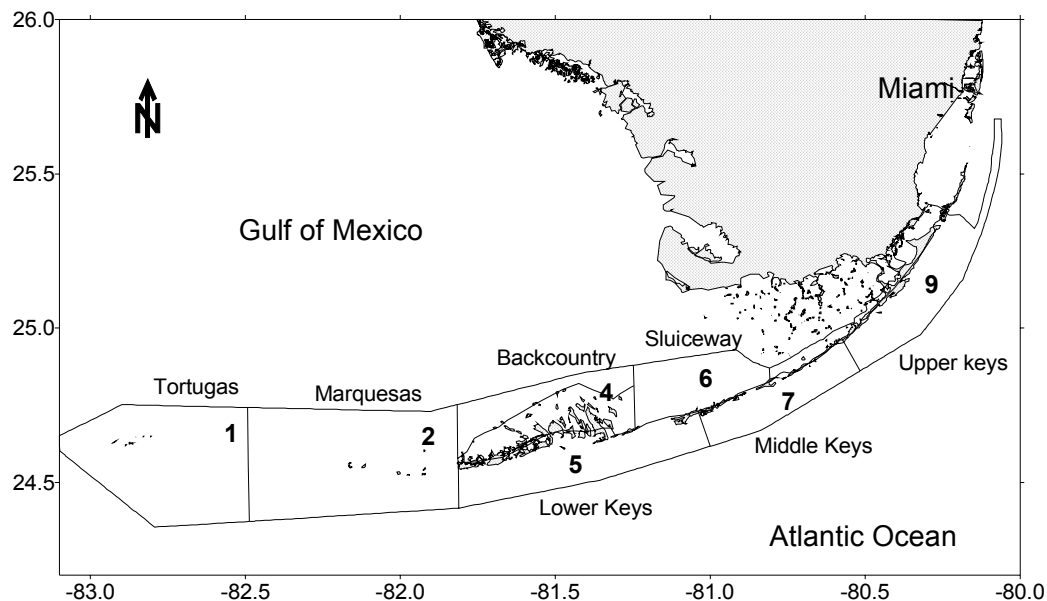


**Figure 1.** Map of South Florida showing FKNMS boundary, Segment numbers, and common names for Segments.

The waters of the FKNMS are characterized by complex water circulation patterns over both spatial and temporal scales with much of this variability due to seasonal influence in regional circulation regimes. The FKNMS is directly influenced by the Florida Current, the Gulf of Mexico Loop Current, inshore currents of the SW Florida Shelf (Shelf), discharge from the Everglades through the Shark River Slough, and by tidal exchange with both Florida Bay and Biscayne Bay (Lee et al. 1994, Lee et al. 2002). Advection from these external sources has

significant effects on the physical, chemical, and biological composition of waters within the FKNMS, as may internal nutrient loading and freshwater runoff from the Keys themselves. Water quality of the FKNMS may be directly affected both by external nutrient transport and internal nutrient loading sources. Therefore, the geographical extent of the FKNMS is one of political/regulatory definition and should not be thought of as an enclosed ecosystem.

A spatial framework for FKNMS water quality management was proposed on the basis of geographical variation of regional circulation patterns (Klein and Orlando, 1994). The final implementation plan (EPA, 1995) partitioned the FKNMS into 9 segments which was collapsed to 7 for routine sampling (Fig. 1). Station locations were developed using a stratified random design along onshore/offshore transects in Segment 5, 7, and 9 or within EMAP grid cells in Segment 1, 2, 4, and 6.

Segment 1 (Tortugas) includes the Dry Tortugas National Park (DTNP) and surrounding waters and is most influenced by the Loop Current and Dry Tortugas Gyre. Originally, there were no sampling sites located within the DTNP as it was outside the jurisdiction of NOAA. Upon request from the National Park Service, we initiated sampling at 5 sites within the DTNP boundary. Segment 2 (Marquesas) includes the Marquesas Keys and a shallow sandy area between the Marquesas and Tortugas called the Quicksands. Segment 4 (Backcountry) contains the shallow, hard-bottomed waters on the gulfside of the Lower Keys. Segments 2 and 4 are both influenced by water moving south along the SW Shelf. Segment 6 can be considered as part of western Florida Bay. This area is referred to as the Sluiceway as it strongly influenced by transport from Florida Bay, SW Shelf, and Shark River Slough (Smith, 1994). Segments 5 (Lower Keys), 7 (Middle Keys), and 9 (Upper Keys) include the inshore, Hawk Channel, and reef tract of the Atlantic side of the Florida Keys. The Lower Keys are most influenced by cyclonic gyres spun off of the Florida Current, the Middle Keys by exchange with Florida Bay, while the Upper Keys are influenced by the Florida Current frontal eddies and to a certain extent by exchange with Biscayne Bay. All three oceanside segments are also influenced by wind and tidally driven lateral Hawk Channel transport (Pitts, 1997).

We have found that water quality monitoring programs composed of many sampling stations situated across a diverse hydroscape are often difficult to interpret due to the “can’t see the forest for the trees” problem (Boyer et al. 2000). At each site, the many measured variables are independently analyzed, individually graphed, and separately summarized in tables. This



approach makes it difficult to see the larger, regional picture or to determine any associations among sites. In order to gain a better understanding of the spatial patterns of water quality of the FKNMS, we attempted to reduce the complicated data matrix into fewer elements which would provide robust estimates of condition and connection. To this end we developed an objective classification analysis procedure which grouped stations according to water quality similarity.

Ongoing quarterly sampling of >200 stations in the FKNMS and Shelf, as well as monthly sampling of 100 stations in Florida Bay, Biscayne Bay, and the mangrove estuaries of the SW coast (Fig.2), has provided us with a unique opportunity to explore the spatial component of water quality variability. By stratifying the sampling stations according to depth, regional geography, distance from shore, proximity to tidal passes, and influence of Shelf waters we report some preliminary conclusions as to the relative importance of external vs. internal factors on the ambient water quality within the FKNMS.

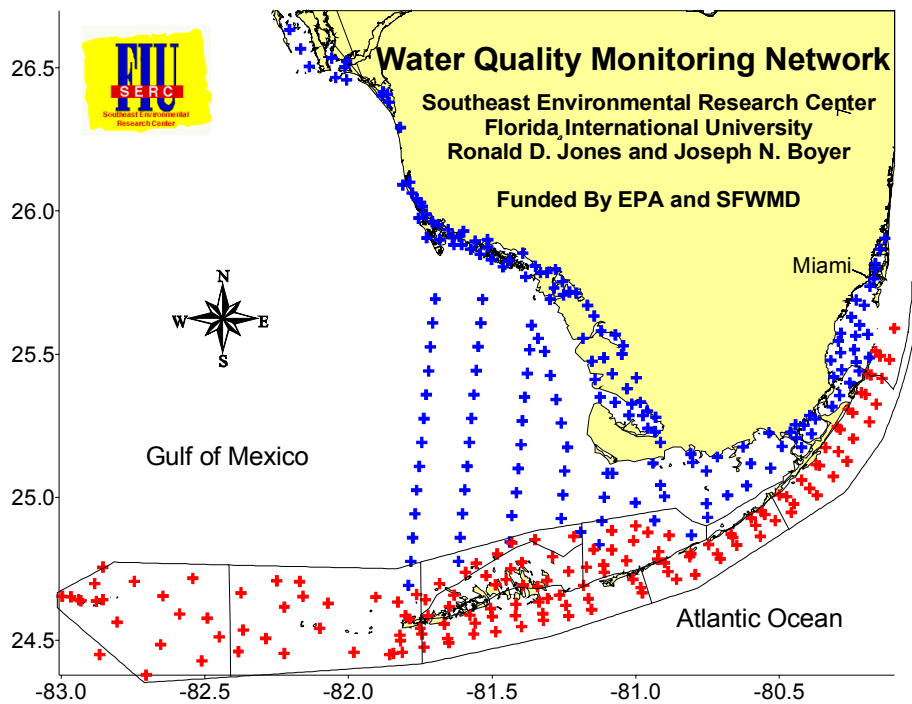


**Figure 2.** The SERC Water Quality Monitoring Network showing the distribution of fixed sampling stations (+) within the FKNMS, Florida Bay, Biscayne Bay, Whitewater Bay, Ten Thousand Islands, and Southwest Florida Shelf.

## II. Methods

### *Field Sampling*

The period of record of this study was from March 1995 to September 2002 which included 29 quarterly sampling events. For each event, field measurements and grab samples were collected from 154 fixed stations within the FKNMS boundary (Fig. 2). Depth profiles of temperature ( $^{\circ}\text{C}$ ), salinity (practical salinity scale), dissolved oxygen (DO,  $\text{mg l}^{-1}$ ), photosynthetically active radiation (PAR,  $\mu\text{E m}^{-2} \text{s}^{-1}$ ), *in situ* chlorophyll *a* specific fluorescence (FSU), optical backscatterance turbidity (OBS), depth as measured by pressure transducer (m), and density ( $\sigma_t$ , in  $\text{kg m}^{-3}$ ) were measured by CTD casts (Seabird SBE 19). The CTD was equipped with internal RAM and operated in stand alone mode at a sampling rate of 0.5 sec. The vertical light attenuation coefficient ( $K_d$ ,  $\text{m}^{-1}$ ) was calculated at 0.5 m intervals from PAR and depth using the standard exponential equation (Kirk 1994) and averaged over the station depth. This was necessary due to periodic occurrence of optically distinct layers within the water column. During these events,  $K_d$  was reported for the upper layer. To determine the extent of stratification we calculated the difference between surface and bottom density as  $\Delta\sigma_t$ , where positive values denoted greater density of bottom water relative to the surface. A  $\Delta\sigma_t > 1$  is weakly stratified, while anything  $> 2$  is considered strongly stratified.

In the Backcountry area (Seg. 4, Fig. 1) where it was too shallow to use a CTD, surface salinity and temperature were measured using a combination salinity-conductivity-temperature probe (Orion model 140). DO was measured using an oxygen electrode (Orion model 840) corrected for salinity and temperature. PAR was measured using a Li-Cor irradiance meter equipped with two  $4\pi$  spherical sensors (LI-193SB) separated by 0.5 m in depth and oriented at  $90^{\circ}$  to each other. The light meter measured instantaneous difference between sensors which was then used to calculate  $K_d$  from in-air surface irradiance.

Water was collected from approximately 0.25 m below the surface and at approximately 1 m from the bottom with a teflon-lined Niskin bottle (General Oceanics) except in the Backcountry and Sluiceway where it was collected directly into sample bottles. Duplicate, unfiltered water samples were dispensed into 3x sample rinsed 120 ml HDPE bottles for analysis of total constituents. Duplicate water samples for dissolved nutrients were dispensed into 3x sample rinsed 150 ml syringes which were then filtered by hand through 25 mm glass fiber filters

(Whatman GF/F) into 3x sample rinsed 60 ml HDPE bottles. The resulting wet filters, used for chlorophyll *a* (CHLA) analysis, were placed in 1.8 ml plastic centrifuge tubes to which 1.5 ml of 90 % acetone/water was added (Strickland and Parsons 1972).

Unfiltered samples were kept at ambient temperature in the dark during transport to the laboratory. During shipboard collection in the Tortugas/Marquesas and overnight stays in the Keys, unfiltered samples were analyzed for APA and turbidity prior to refrigeration. Filtered samples and CHLA filters were kept on ice in the dark during transport. During shipboard collection in the Tortugas/Marquesas and overnight stays in the lower Keys, filtrates and filters were frozen until further analysis.

### Laboratory Analysis

Unfiltered water samples were analyzed for total organic carbon (TOC), total nitrogen (TN), total phosphorus (TP), silicate ( $\text{Si}(\text{OH})_4$ ), alkaline phosphatase activity (APA), and turbidity. TOC was measured by direct injection onto hot platinum catalyst in a Shimadzu TOC-5000 after first acidifying to  $\text{pH} < 2$  and purging with  $\text{CO}_2$ -free air. TN was measured using an ANTEK 7000N Nitrogen Analyzer using  $\text{O}_2$  as carrier gas to promote complete recovery of the nitrogen in the water samples (Frankovich and Jones 1998). TP was determined using a dry ashing, acid hydrolysis technique (Solórzano and Sharp 1980).  $\text{Si}(\text{OH})_4$  was measured using the molybdosilicate method (Strickland and Parsons 1972). The APA assay measures the activity of alkaline phosphatase, an enzyme used by bacteria and algae to mineralize orthophosphate from organic compounds. The assay is performed by adding a known concentration of methylfluorescein phosphate to an unfiltered water sample. Alkaline phosphatase in the water sample cleaves the orthophosphate, leaving methylfluorescein, a highly fluorescent compound. Fluorescence at initial and after 2 hr incubation were measured using a Gilford Fluoro IV Spectrofluorometer (excitation = 430 nm, emission = 507 nm) and subtracted to give APA in  $\mu\text{M h}^{-1}$  (Jones 1996). Turbidity was measured using an HF Scientific model DRT-15C turbidimeter and reported in NTU.

Filtrates were analyzed for nitrate+nitrite ( $\text{NO}_x^-$ ), nitrite ( $\text{NO}_2^-$ ), ammonium ( $\text{NH}_4^+$ ), and soluble reactive phosphorus (SRP) by flow injection analysis (Alpkem model RFA 300). Filters for CHLA content ( $\mu\text{g l}^{-1}$ ) were allowed to extract for a minimum of 2 days at  $-20^\circ\text{C}$  before analysis. Extracts were analyzed using a Gilford Fluoro IV Spectrofluorometer (excitation = 435

nm, emission = 667 nm). All analyses were completed within 1 month after collection in accordance to SERC laboratory QA/QC guidelines.

Some parameters were not measured directly, but were calculated by difference. Nitrate ( $\text{NO}_3^-$ ) was calculated as  $\text{NO}_X^- - \text{NO}_2^-$ , dissolved inorganic nitrogen (DIN) as  $\text{NO}_X^- + \text{NH}_4^+$ , and total organic nitrogen (TON) defined as  $\text{TN} - \text{DIN}$ . All concentrations are reported as  $\mu\text{M}$  unless noted. All elemental ratios discussed were calculated on a molar basis. DO saturation in the water column ( $\text{DO}_{\text{sat}}$  as %) was calculated using the equations of Garcia and Gordon (1992).

### Objective Classification Analysis

Stations were stratified according to water quality characteristics (i.e. physical, chemical, and biological variables) using a statistical approach. Multivariate statistical techniques have been shown to be useful in reducing a large data sets into a smaller set of independent, synthetic variables that capture much of the original variance. The method we chose was a type of objective classification analysis (OCA) which uses principal component analysis (PCA) followed by k-means clustering algorithm to classify sites as to their overall water quality. This approach has been very useful in understanding the factors influencing nutrient biogeochemistry in Florida Bay (Boyer et al., 1997), Biscayne Bay, and the Ten Thousand Islands (Boyer and Jones, 1998). We have found that water quality at a specific site is the result of the interaction of a variety of driving forces including oceanic and freshwater inputs/outputs, sinks, and internal cycling.

Briefly, data were first standardized as Z-scores prior to analysis to reduce artifacts of differences in magnitude among variables. PCA was used to extract statistically significant composite variables (principal components) from the original data (Overland and Preisendorfer 1982). The PCA solution was rotated (using VARIMAX) in order to facilitate the interpretation of the principal components and the factor scores were saved for each data record. Both the mean and SD of the factor scores for each station over the entire period of record were then used as independent variables in a cluster analysis (k-means algorithm) in order to aggregate stations into groups of similar water quality. The purpose of this analysis was to collapse the 154 stations into a few groups which could then be analyzed in more detail.

### Box and Whisker Plots

Typically, water quality data are skewed to the left (low concentrations and below detects) resulting in non-normal distributions. Therefore it is more appropriate to use the median as the measure of central tendency because the mean is inflated by high outliers (Christian et al. 1991). Data distributions of water quality variables are reported as box-and-whiskers plots. The box-and-whisker plot is a powerful statistic as it shows the median, range, the data distribution as well as serving as a graphical, nonparametric ANOVA. The center horizontal line of the box is the median of the data, the top and bottom of the box are the 25<sup>th</sup> and 75<sup>th</sup> percentiles (quartiles), and the ends of the whiskers are the 5<sup>th</sup> and 95<sup>th</sup> percentiles. The notch in the box is the 95% confidence interval of the median. When notches between boxes do not overlap, the medians are considered significantly different. Outliers (<5<sup>th</sup> and >95<sup>th</sup> percentiles) were excluded from the graphs to reduce visual compression. Differences in variables were also tested between groups using the Wilcoxon Ranked Sign test (comparable to a *t*-test) and among groups by the Kruskal-Wallis test (ANOVA) with significance set at  $P < 0.05$ .

### Contour Maps

In an effort to elucidate the contribution of external factors to the water quality of the FKNMS and to visualize gradients in water quality over the region, we combined data from other portions of our water quality monitoring network: Florida Bay, Biscayne Bay, Whitewater Bay, Ten Thousand Islands, SW Shelf, and Marco Island – Ft. Meyers (see example in Fig. 10 and <http://serc.fiu.edu/wqmnetwork/CONTOUR%20MAPS/ContourMaps.htm> for all other maps). Data from these 153 additional stations were collected during the same month as the FKNMS surveys and analyzed by the SERC laboratory using identical methods. Contour maps were produced using Surfer (Golden Software). The most important aspect of generating contour maps is the geostatistical algorithm used for interpolating the data values. Care should be taken in the selection of the algorithm because automated interpolation to a regular rectangular grid can produce artifacts, especially around the edges and when the area of interest is irregularly shaped. The kriging algorithm was used because it is designed to minimize the error variance while at the same time maintaining point pattern continuity (Isaaks & Srivastava, 1989). Kriging is a global approach which uses standard geostatistics to determine the "distance" of influence around each point and the "clustering" of similar samples sites

(autocorrelation). Therefore, unlike the inverse distance procedure, kriging will not produce valleys in the contour between neighboring points of similar value.

### *Time Series Analysis*

Individual site data for the complete period of record were plotted as time series graphs (see <http://serc.fiu.edu/wqmnetwork/CONTOUR%20MAPS/ContourMaps.htm>) to illustrate any temporal trends that might have occurred. Temporal trends were quantified by simple regression with significance set at  $P < 0.05$ . We originally planned to use a seasonal Kendall- $\tau$  analysis to test for monotonic trend (Hirsch et al. 1991) but found that it was not yet applicable to this short, quarterly sampled data set.

### III. Results

#### General Water Quality of the FKNMS

Summary statistics for all water quality variables from all 29 sampling events are shown as median, minimum, maximum, and number of samples (Table 1). Overall, the region was warm and euhaline with a median temperature of 27.1°C and salinity of 36.2; oxygen saturation of the water column ( $DO_{\text{sat}}$ ) was relatively high at 90.1%. On this coarse scale, the FKNMS exhibited very good water quality with median  $\text{NO}_3^-$ ,  $\text{NH}_4^+$ , and TP concentrations of 0.09, 0.30, and 0.20  $\mu\text{M}$ , respectively.  $\text{NH}_4^+$  was the dominant DIN species in almost all of the samples (~70 %). However, DIN comprised a small fraction (4 %) of the TN pool with TON making up the bulk (median 10.3  $\mu\text{M}$ ). SRP concentrations were very low (median 0.013  $\mu\text{M}$ ) and comprised only 6 % of the TP pool. CHLA concentrations were also very low overall, 0.26  $\mu\text{g l}^{-1}$ , but ranged from 0.01 to 15.2  $\mu\text{g l}^{-1}$ . TOC was 199.7; a value higher than open ocean levels but consistent with coastal areas. Median turbidity was low (0.6 NTU) as reflected in a low  $K_d$  (0.23  $\text{m}^{-1}$ ). This resulted in a median photic depth (to 1 % incident PAR) of ~22 m. Molar ratios of N to P suggested a general P limitation of the water column (median TN:TP = 57, not shown) but this must be tempered by the fact that much of the TN is not bioavailable.

**Table 1.** Summary statistics for each water quality variable in the FKNMS for the period of record. Data are summarized as median (Median), minimum value (Min.), maximum value (Max.), and number of samples ( $n$ ).

| Variable                             | Depth   | Median | Min.  | Max.    | $n$  |
|--------------------------------------|---------|--------|-------|---------|------|
| $\text{NO}_3^-$<br>( $\mu\text{M}$ ) | Surface | 0.087  | 0.000 | 5.902   | 4386 |
|                                      | Bottom  | 0.080  | 0.000 | 5.010   | 2675 |
| $\text{NO}_2^-$<br>( $\mu\text{M}$ ) | Surface | 0.043  | 0.000 | 0.710   | 4396 |
|                                      | Bottom  | 0.038  | 0.000 | 1.732   | 2682 |
| $\text{NH}_4^+$<br>( $\mu\text{M}$ ) | Surface | 0.299  | 0.000 | 10.320  | 4395 |
|                                      | Bottom  | 0.268  | 0.000 | 3.876   | 2680 |
| TN<br>( $\mu\text{M}$ )              | Surface | 10.830 | 1.707 | 211.095 | 4391 |
|                                      | Bottom  | 9.036  | 1.482 | 152.231 | 2661 |
| TON<br>( $\mu\text{M}$ )             | Surface | 10.261 | 0.389 | 210.778 | 4372 |
|                                      | Bottom  | 8.445  | 0.000 | 151.909 | 2641 |
| TP<br>( $\mu\text{M}$ )              | Surface | 0.198  | 0.000 | 1.777   | 4394 |
|                                      | Bottom  | 0.185  | 0.000 | 1.497   | 2663 |

| <b>Variable</b>                                | <b>Depth</b> | <b>Median</b> | <b>Min.</b> | <b>Max.</b> | <b>n</b> |
|--|--------------|---------------|-------------|-------------|----------|
| <b>SRP</b><br>( $\mu\text{M}$ )                | Surface      | 0.013         | 0.000       | 0.297       | 4383     |
|  | Bottom       | 0.013         | 0.000       | 0.390       | 2674     |
| <b>APA</b><br>( $\mu\text{M h}^{-1}$ )         | Surface      | 0.060         | 0.000       | 5.616       | 4232     |
|  | Bottom       | 0.048         | 0.000       | 0.491       | 2520     |
| <b>CHLA</b> ( $\mu\text{g l}^{-1}$ )           | Surface      | 0.261         | 0.010       | 15.239      | 4394     |
| <b>TOC</b><br>( $\mu\text{M}$ )                | Surface      | 199.69        | 83.77       | 1653.54     | 4393     |
|  | Bottom       | 171.60        | 89.38       | 883.10      | 2669     |
| <b>Si(OH)<sub>4</sub></b><br>( $\mu\text{M}$ ) | Surface      | 0.701         | 0.000       | 127.110     | 4090     |
|  | Bottom       | 0.455         | 0.000       | 30.195      | 2491     |
| <b>Turbidity</b><br>(NTU)                      | Surface      | 0.62          | 0.00        | 37.00       | 4349     |
|  | Bottom       | 0.52          | 0.00        | 16.90       | 2700     |
| <b>Salinity</b>                                | Surface      | 36.2          | 26.7        | 40.9        | 4315     |
|  | Bottom       | 36.2          | 27.7        | 40.9        | 4287     |
| <b>Temperature</b><br>( $^{\circ}\text{C}$ )   | Surface      | 27.1          | 15.1        | 39.6        | 4322     |
|  | Bottom       | 26.6          | 15.1        | 36.8        | 4294     |
| <b>K<sub>d</sub></b> ( $\text{m}^{-1}$ )       |              | 0.230         | 0.003       | 3.410       | 3050     |
| <b>DO<sub>sat</sub></b><br>(%)                 | Surface      | 90.1          | 31.2        | 191.6       | 4286     |
|  | Bottom       | 89.9          | 19.3        | 207.0       | 4240     |
| <b><math>\Delta\sigma_t</math></b>             |              | 0.007         | -4.424      | 6.640       | 4269     |

### Objective Classification Analysis

PCA identified five composite variables (hereafter called PC1, PC2, etc.) that passed the rule N for significance at  $P < 0.05$  (Overland and Preisendorfer 1982) indicating five separate modes of variation in the data (Table 2). These five principal components accounted for 63.2 % of the total variance of the original variables. PC1 had high factor loadings for  $\text{NO}_3^-$ ,  $\text{NO}_2^-$ ,  $\text{NH}_4^+$ , and SRP and was named the “Inorganic Nutrient” component. PC2 included TP, APA, CHLA, and turbidity and was designated as the “Phytoplankton” component. The covariance of TP with CHLA implies that, in many areas, phytoplankton biomass may be limited by phosphorus availability. This is contrary to much of the literature on the subject which usually ascribes nitrogen as being the limiting factor for phytoplankton production in coastal oceans. TON and TOC were included in PC3 as the “Terrestrial Organic” component. Temperature and DO were inversely related in PC4. Finally, PC5 included salinity and TP, implying a source of TP from marine waters. Note that TP had two modes of variability as a function of its distribution.



**Table 2.** Results of principal component analysis are shown as factor loadings (correlations between the raw variables and the principal components) for the first four principal components after VARIMAX rotation. For clarity, loadings with a magnitude >0.450 are shown in boldface type.

| <b>Variable</b>                   | <b>PC1</b>   | <b>PC2</b>   | <b>PC3</b>   | <b>PC4</b>    | <b>PC5</b>   |
|-----------------------------------|--------------|--------------|--------------|---------------|--------------|
| <b>NO<sub>3</sub><sup>-</sup></b> | <b>0.707</b> | 0.094        | -0.121       | 0.100         | 0.004        |
| <b>NO<sub>2</sub><sup>-</sup></b> | <b>0.608</b> | -0.082       | 0.354        | 0.057         | 0.111        |
| <b>NH<sub>4</sub><sup>+</sup></b> | <b>0.691</b> | -0.124       | 0.200        | 0.001         | -0.087       |
| <b>TON</b>                        | 0.001        | 0.071        | <b>0.720</b> | -0.139        | 0.126        |
| <b>TP/TP</b>                      | 0.220        | <b>0.449</b> | -0.047       | -0.414        | <b>0.499</b> |
| <b>SRP</b>                        | <b>0.550</b> | 0.245        | -0.413       | -0.037        | -0.112       |
| <b>APA</b>                        | -0.066       | <b>0.693</b> | 0.214        | 0.394         | 0.041        |
| <b>CHLA</b>                       | 0.001        | <b>0.789</b> | -0.135       | 0.006         | -0.217       |
| <b>TOC</b>                        | 0.038        | 0.073        | <b>0.696</b> | 0.089         | -0.185       |
| <b>Turbidity</b>                  | 0.036        | <b>0.591</b> | 0.190        | -0.261        | 0.040        |
| <b>Salinity</b>                   | -0.108       | -0.141       | -0.010       | 0.201         | <b>0.820</b> |
| <b>Temp.</b>                      | -0.001       | -0.001       | 0.141        | <b>0.802</b>  | 0.074        |
| <b>DO</b>                         | -0.122       | 0.052        | 0.109        | <b>-0.737</b> | -0.024       |
| %Variance                         |              |              |              |               |              |
| Explained                         | 19.0         | 16.2         | 10.6         | 9.5           | 7.9          |

Spatial distributions of the mean factor score for each station indicated how the average water quality varied over the study area. The “Inorganic Nutrient” component had two peaks: in the Backcountry and bayside of the Middle Keys. The “Phytoplankton” component described a N to S gradient in the Backcountry and Sluiceway which extended west across the northern Marquesas. The “Terrestrial Organic” component was highest in eastern Sluiceway extending into the Backcountry and was also distributed as a gradient away from land on the Atlantic side of the Keys. Temperature and DO showed a distribution heavily loaded in the oceanside. Finally the salinity/TP component showed lower loadings in the alongshore Upper Keys and bayside Sluiceway extending through most Atlantic sites of the Middle and Lower Keys.

The k-means clustering algorithm used the mean and SD of the four factor scores of each station to classify all 150 sampling sites into 8 groups having robust correspondence in water quality (Fig. 3). The bulk of the stations fell into 6 large clusters (1, 3, 5, 6, 7, and 8) which described a gradient of water quality throughout the FKNMS. Although the differences among them were very subtle, they were statistically significant and allowed us to say that the overall

nutrient gradient, from highest to lowest concentrations, was cluster 7, 8>1>5>6>3 (Table 3 in Appendix).

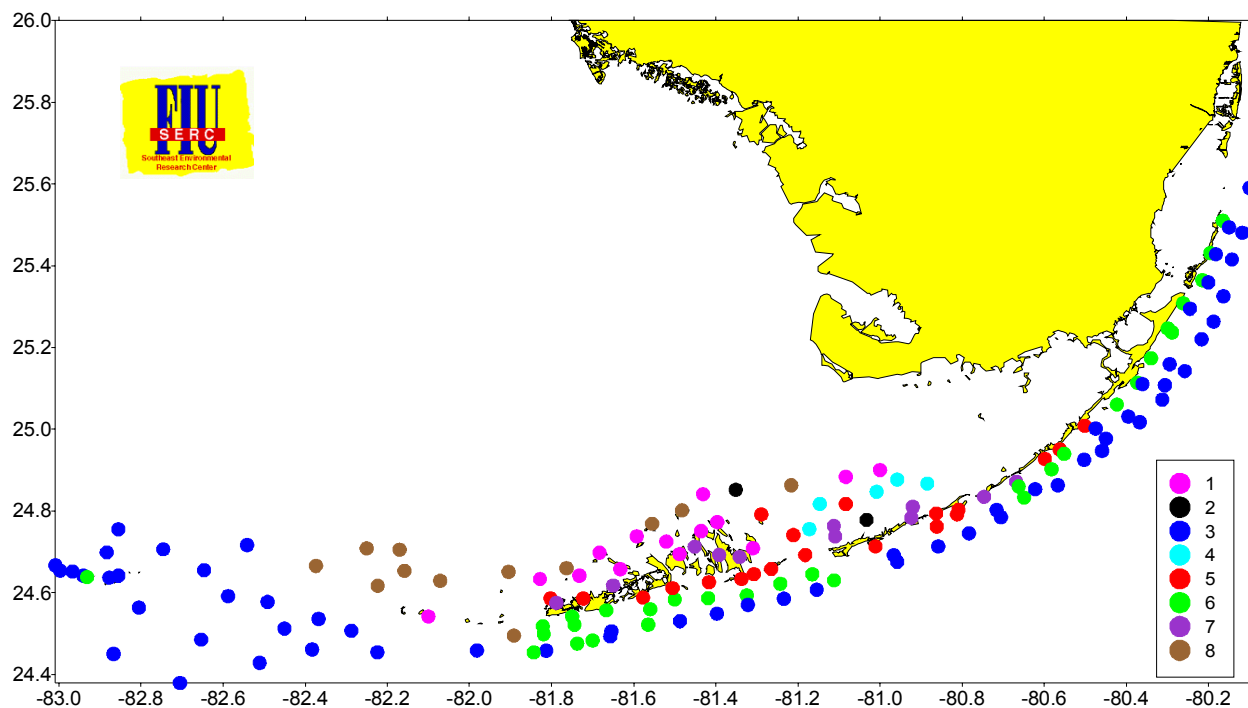


**Figure 3.** Results of objective analysis showing station membership in distinct water quality groups.

Cluster 7 (●) was composed primarily stations located inside the Backcountry, bayside Middle Keys, and the inshore sites off Lower Matecumbe Key. This group was highest in inorganic nutrients, especially  $\text{NO}_3^-$ , as well as TOC and TON (Fig. 4). We expect that there are different reasons for the distribution of these sites. In the shallow Backcountry sites we expect that benthic flux of nutrients might be very important, whereas elevated DIN at inshore Lower Matecumbe sites may be the result of anthropogenic loading.

Cluster 8 (●) included the northernmost sites in the Sluiceway, Backcountry and Marquesas. It had the highest TP, CHLA, and turbidity but was low in inorganic nutrients, DON, and DOC. We believe that the water quality in Cluster 8 was primarily driven by Shelf circulation patterns.

Cluster 1 (●) was composed of 2 sites in the northern Sluiceway and 12 sites in northern Backcountry extending out to the Marquesas. This group was high in TP, CHLA, and turbidity. The main distinction between Cluster 1 and 8 was higher in CHLA and lower in TOC. So Clusters 8 and 1 may be viewed as a gradient of high TP Shelf water being attenuated by uptake of nutrients within the Backcountry and/or mixing with Atlantic Ocean waters.

Clusters 5, 6, and 3 may be interpreted as representing an onshore-offshore nutrient gradient. Cluster 5 (●) included the most of the inshore sites of the Keys, excluding the northernmost and southernmost ones. They were elevated in DIN relative to the Hawk Channel and reef tract sites. Cluster 6 (●) was made up of sites in Hawk Channel of the Lower Keys and alongshore sites in the Upper Keys. This group was slightly lower in nutrients than Cluster 5. Cluster 3 (●) was made up of outer reef tract and Tortugas stations. These sites had lowest nutrients, CHLA, turbidity, and TOC of any in the FKNMS. A clear gradient of elevated DIN, TP, TOC, and turbidity from alongshore to offshore was observed in the Keys with the Upper Keys being lower than the Middle and Lower Keys. No significant onshore-offshore gradient was observed for CHLA.

Sites making up Cluster 4 (●) were located in the Sluiceway and were similar to other Sluiceway sites except that they had the greatest range in salinity. Cluster 2 (●) was composed of only 2 sites in the Sluiceway and will not be discussed.

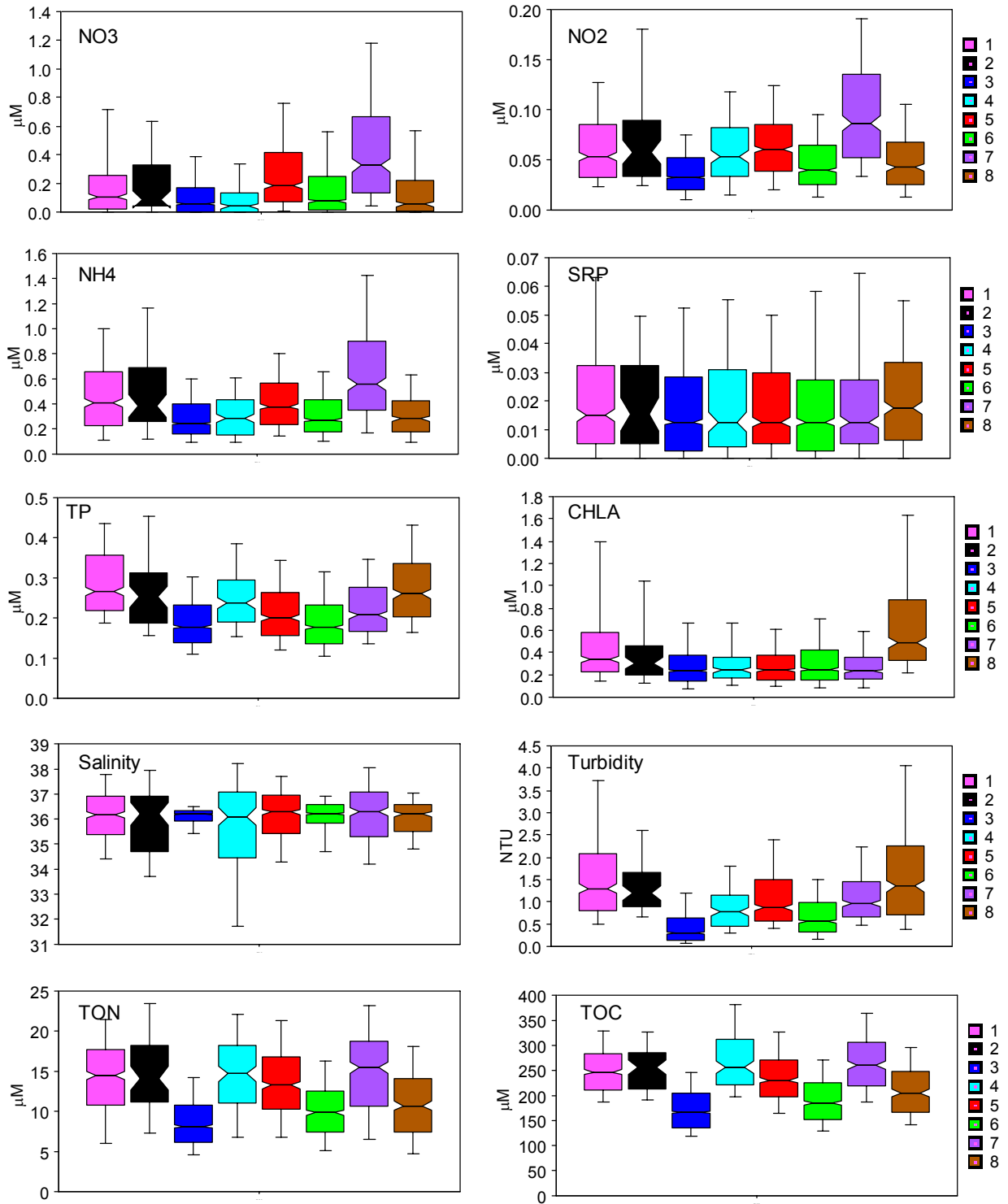


**Figure 4.** Box-and-whisker plots showing median and distribution of NO<sub>3</sub><sup>-</sup>, NO<sub>2</sub><sup>-</sup>, NH<sub>4</sub><sup>+</sup>, SRP, TP, CHLA, salinity, turbidity, TP, TON, and TOC stratified by water quality cluster. Notches in the box that do not overlap with another are considered significantly different.

### Contour Maps

All contour maps of combined data from SFWMD and EPA projects are archived on the website <http://serc.fiu.edu/wqmnetwork/CONTOUR%20MAPS/ContourMaps.htm> and are updated quarterly. An example of such (Fig. 5) shows the distribution of salinity across the region. Both freshwater sources and marine influences are visible using this approach.

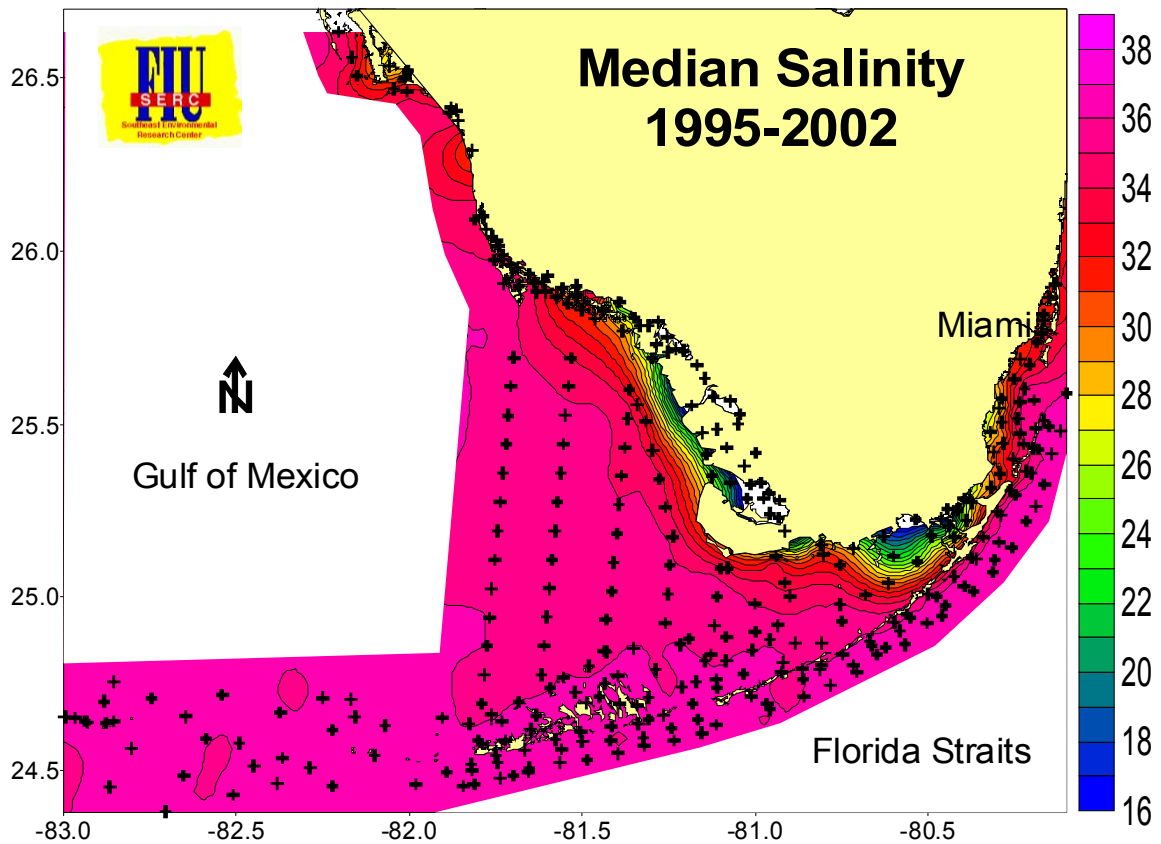


**Figure 5.** Example of contour map of salinity in the region showing freshwater source inputs and marine influences.

### Time Series Analysis

Previously, we observed significant increasing trends in TP,  $\text{NO}_3^-$ , and decreasing TON (Jones and Boyer 2001). We ascribed these trends as being driven primarily by large scale circulation patterns. Since then, there have been trend reversals in some nutrient concentrations. Figures 5-10 show temporal trends in the median and range of the data (box-and-whisker plots) for each group by quarterly sampling event.

The outer reef tract/Tortugas sites (**Cluster 3**) showed large increases in  $\text{NO}_3^-$  and SRP during late 1999 through 2000 (Fig 5). Concurrent with these increases was an increase in CHLA and drop in  $\text{DO}_{\text{sat}}$ . These parameters have since returned to earlier levels. As reported previously, TP was increasing fairly consistently prior to 2001 but have since declined. An interesting aspect of this is that, more than the actual concentration, the variability of TP has increased dramatically. We observed an increased in TON values during 2002 which looks to have returned to previous levels. TOC shows interannual cycles with  $\sim 2$  year period. Salinity is relatively constant except for low salinity excursions due to transport of Shelf waters through the Tortugas Channel and advective transport along the coast by regular gyre formations.

**Cluster 6**, the inshore Upper Keys/Hawk Channel Lower Keys, mirrored the patterns seen in **Cluster 3** except that the concentrations were higher for the nearshore sites (Fig. 6). This implies that the inorganic nutrients did not originate from offshore sources (upwelling). In fact, looking at all the data during this time period showed elevated  $\text{NO}_3^-$  concentrations occurred across the region (Fig. 5-10). This brings up an important point that, when looking at what are perceived to be local trends, we find that they may occur across the whole region at more subtle levels. This spatial autocorrelation in water quality is an inherent property of interconnected systems such as coastal and estuarine ecosystems which are driven by hydrological and climatological forcing.

Clearly, there have been large changes in the FKNMS water quality over time, but no sustained monotonic trends have been observed. We must always keep in mind that trend analysis is limited to the window of observation; trends may change with additional data collection.

### Cluster 3 – Reef Tract/Tortugas

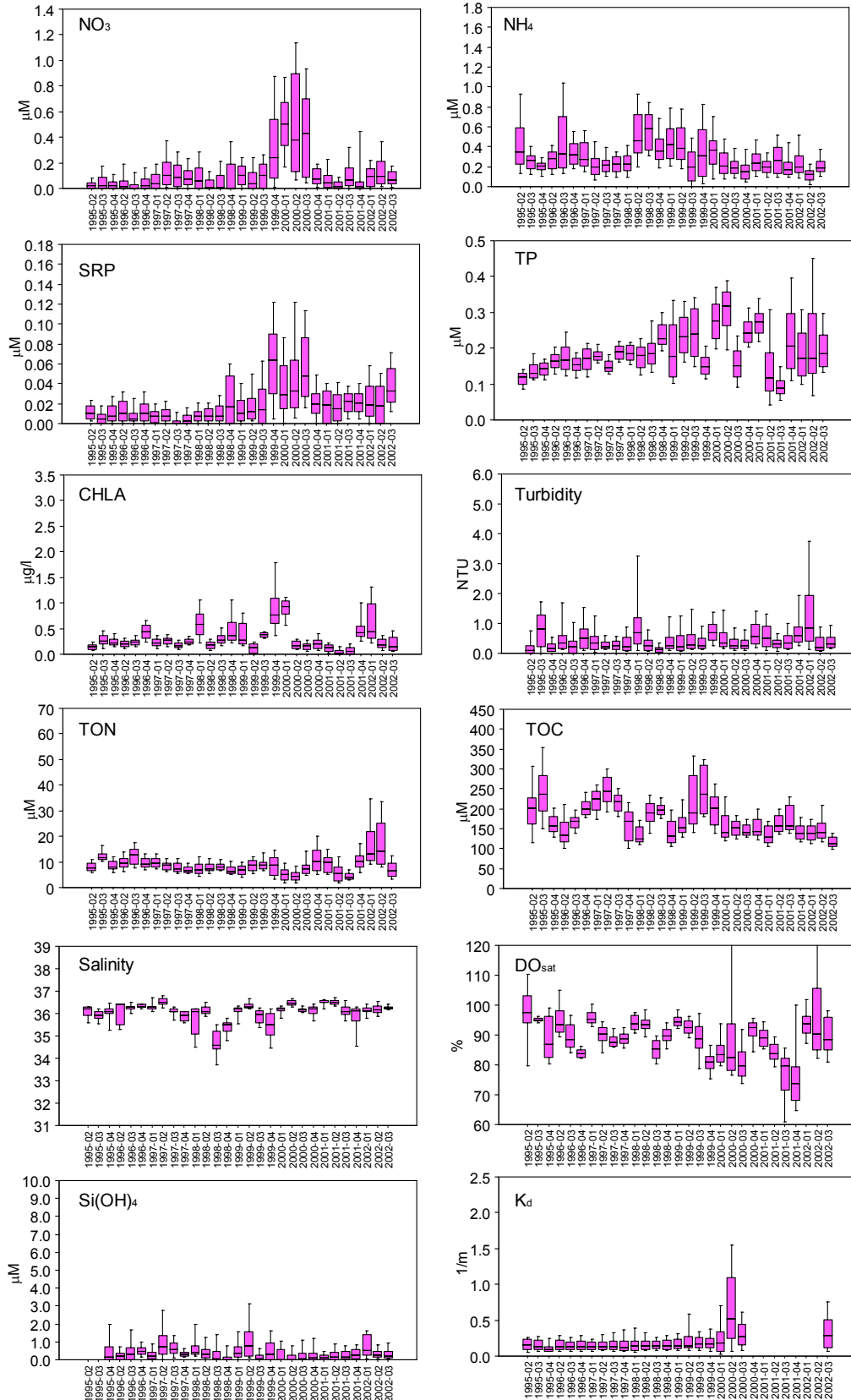


Figure 5.

### Cluster 6 – Inshore Upper Keys/Hawk Channel Lower Keys

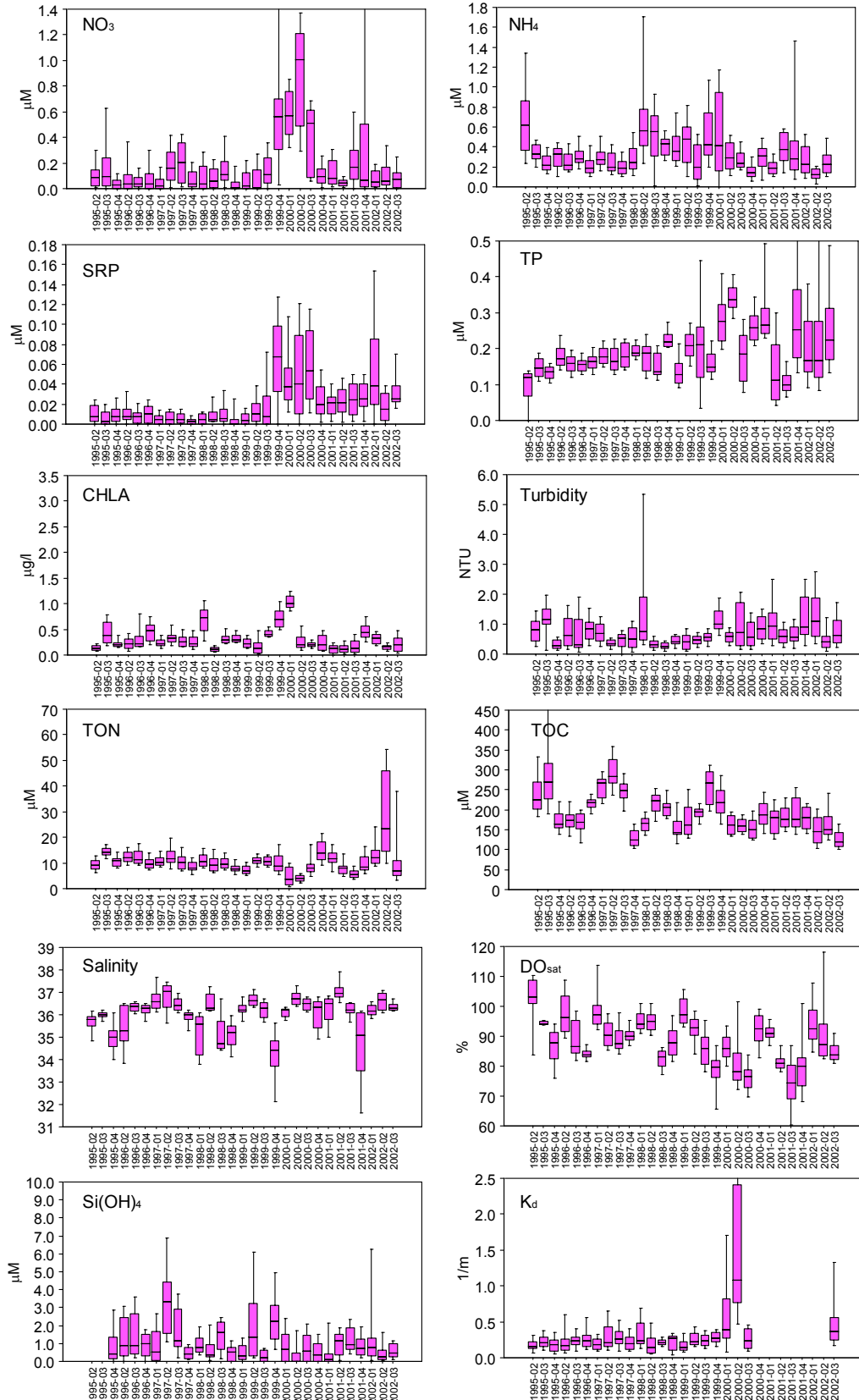


Figure 6.



### Cluster 5 – Inshore Middle and Lower Keys/Sluiceway

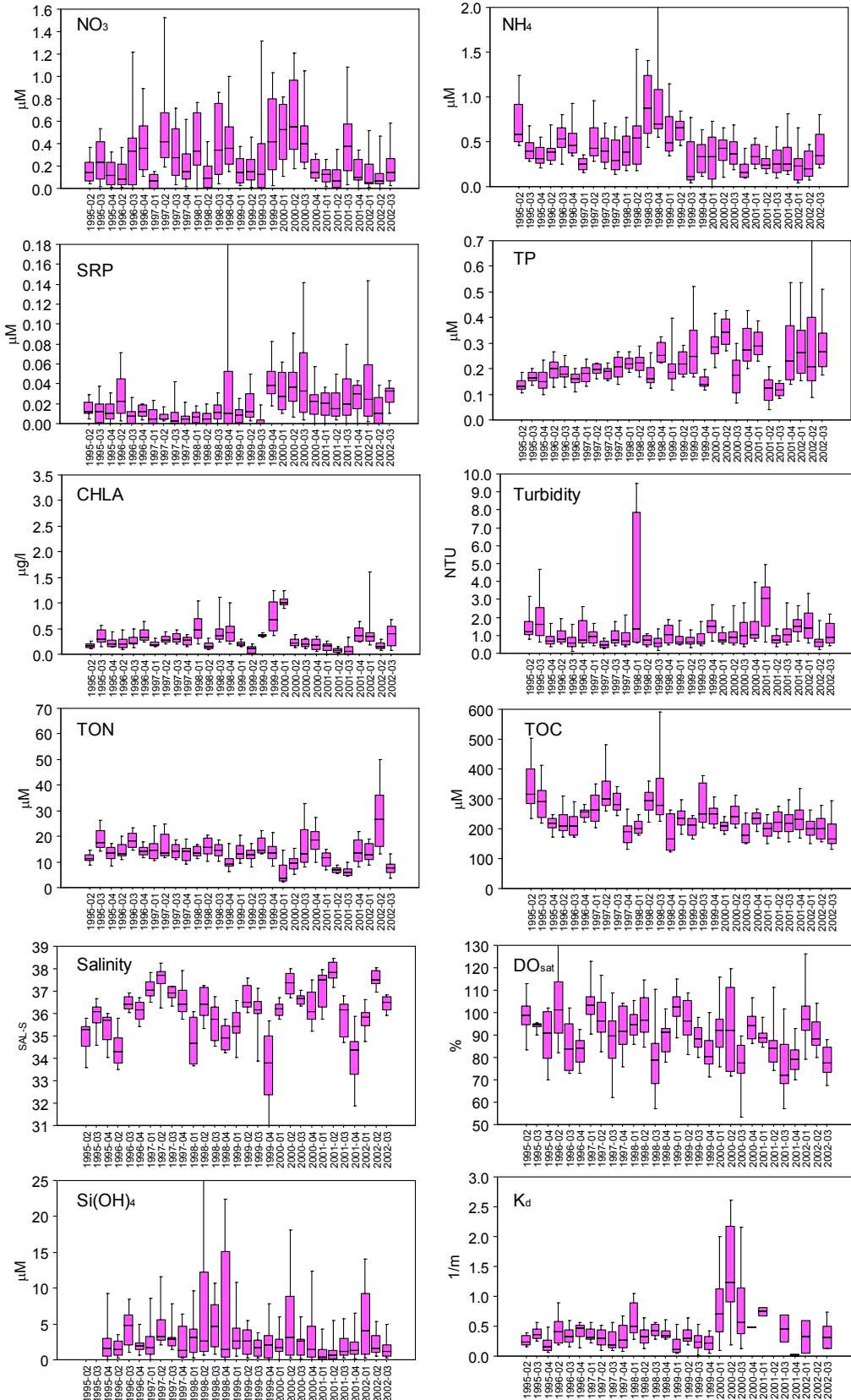


Figure 7.

## Cluster 7 – Bayside Middle Keys/Inside Backcountry/Inshore Long & Lower Matecumbe

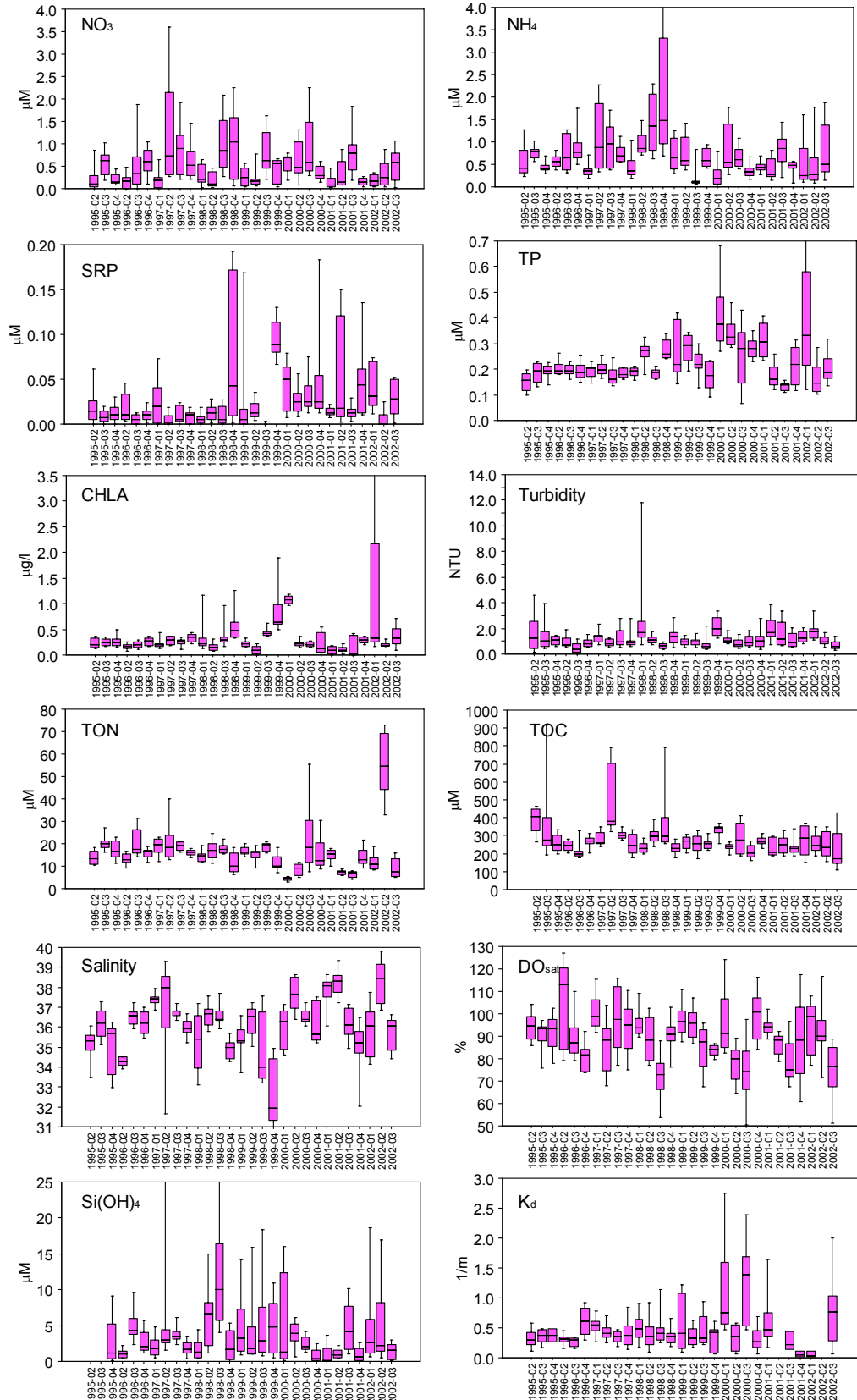


Figure 8.

### Cluster 1 – Backcountry/North Sluiceway

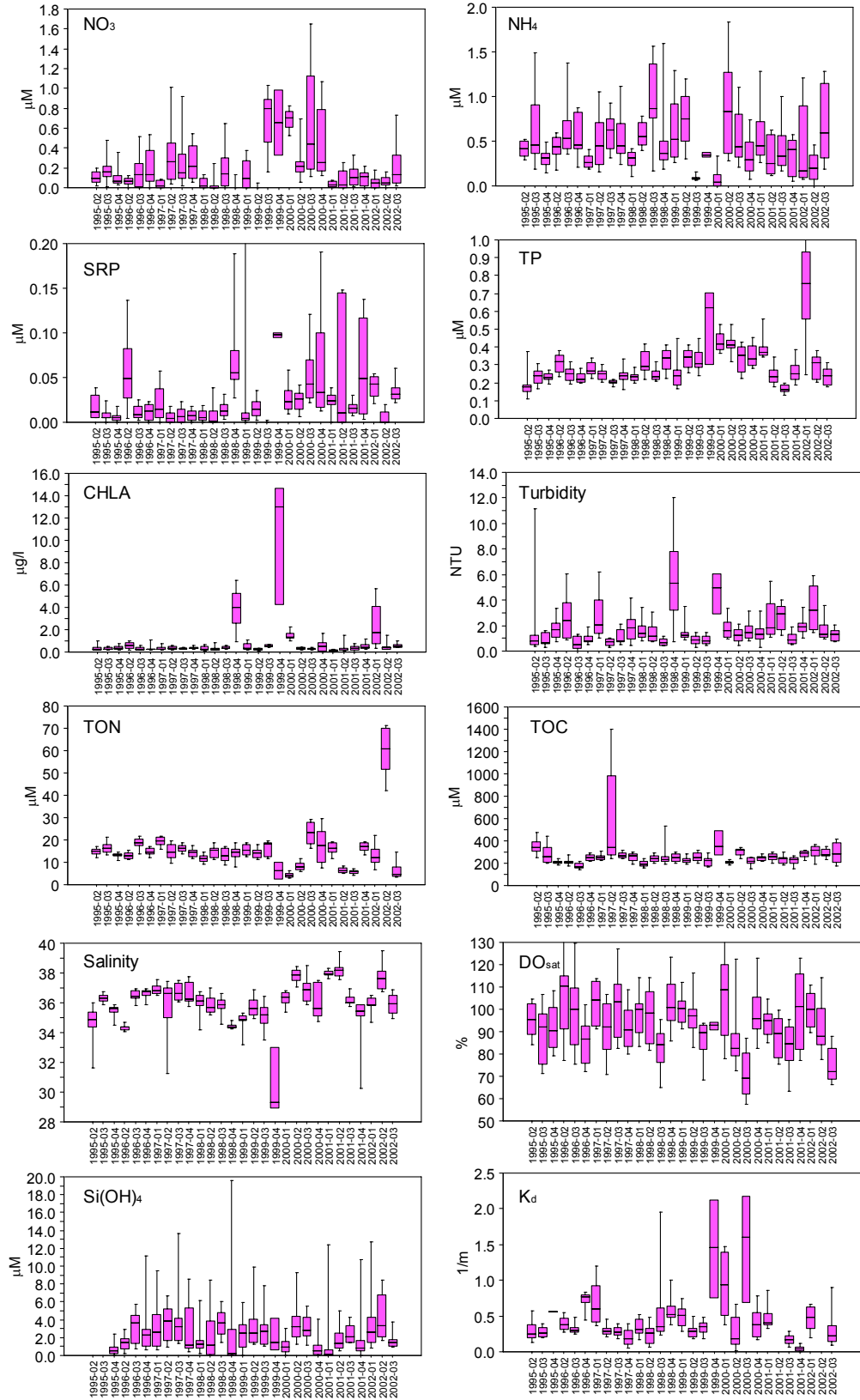


Figure 9.

### Cluster 8– North Marquesas/North Backcountry

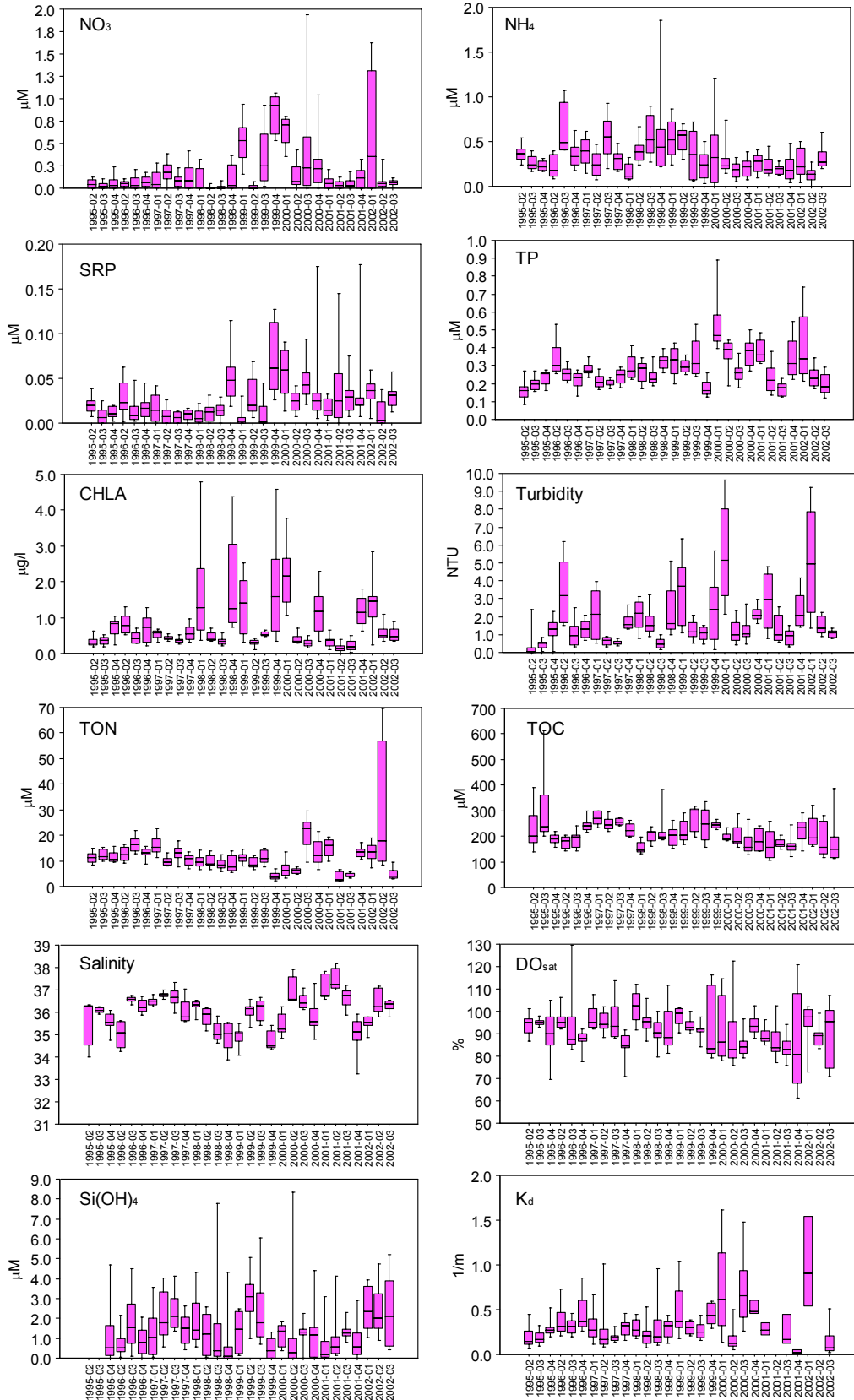


Figure 10.

## IV. Discussion

Water quality is a subjective measure of ecosystem well being. Aside from the physical-chemical composition of the water there is also a human perceptual element which varies according to our intents for use (Kruczyinski and McManus 2002). Distinguishing internal from external sources of nutrients in the FKNMS is a difficult task. The finer discrimination of internal sources into natural and anthropogenic inputs is even more difficult. Most of the important anthropogenic inputs are regulated and most likely controlled by management activities, however, recent studies have shown that nutrients from shallow sewage injection wells may be leaking into nearshore surface waters (Corbett et al. 1999). Advective transport of nutrients through the FKNMS was not measured by the existing fixed sampling plan. However, nutrient distribution patterns may be compared to the regional circulation regimes in an effort to visualize the contribution of external sources and advective transport to internal water quality of the FKNMS.

Circulation in coastal South Florida is dominated by regional currents such as the Loop Current, Florida Current, and Tortugas Gyre and by local transport via Hawk Channel and along-shore Shelf movements (Klein and Orlando 1994). Regional currents may influence water quality over large areas by the advection of external surface water masses into and through the FKNMS (Lee et al. 1994, Lee et al. 2002) and by the intrusion of deep offshore ocean waters onto the reef tract as internal bores (Leichter et al. 1996). Local currents become more important in the mixing and transport of freshwater and nutrients from terrestrial sources (Smith 1994; Pitts 1997).

Spatial patterns of salinity in coastal South Florida show these major sources of freshwater to have more than just local impacts (Fig. 3 and <http://serc.fiu.edu/wqmnetwork/CONTOUR%20MAPS/ContourMaps.htm>). In Biscayne Bay, freshwater is released through the canal system operated by the South Florida Water Management District; the impact is clearly seen to affect northern Key Largo by causing episodic depressions in salinity at alongshore sites. Freshwater entering NE Florida Bay via overland flow from Taylor Slough and C-111 basin mix in a SW direction. The extent of influence of freshwater from Florida Bay on alongshore salinity in the Keys is less than that of Biscayne Bay but it is more episodic. Transport of low salinity water from Florida Bay does not

affect the Middle Keys sites enough to depress the median salinity in this region but is manifested as increased variability. On the west coast, the large influence of the Shark River Slough, which drains the bulk of the Everglades and exits through the Whitewater Bay - Ten Thousand Islands mangrove complex, is clearly seen to impact the Shelf waters. The mixing of Shelf waters with the Gulf of Mexico produces a salinity gradient in a SW direction which extends out to Key West. This freshwater source does not affect the Backcountry because of its shallow nature but instead follows a trajectory of entering western Florida Bay and exiting out through the channels in the Middle Keys (Smith 1994). This net transport of lower salinity water from mainland to reef in open channels through the Keys is observed as an increase in the range and variability of salinity rather than as a large depression in salinity.

In addition to surface currents there is evidence that internal tidal bores regularly impact the Key Largo reef tract (Leichter et al. 1996; Leichter and Miller 1999). Internal bores are episodes of higher density, deep water intrusion onto the shallower shelf or reef tract. Depending on their energy, internal tidal bores can promote stratification of the water column or cause complete vertical mixing as a breaking internal wave of subthermocline water. According to  $\Delta\sigma_t$ , the SW area of the Tortugas segment tends to experience the greatest frequency of stratification events. The decreased temperature and increased salinity in bottom waters from intrusion of deeper denser oceanic waters to this region may also account for increases in  $\text{NO}_3^-$ , TP, and SRP in these bottom waters as well.

Surface  $\text{Si(OH)}_4$  concentrations exhibited a pattern similar to salinity. The source of  $\text{Si(OH)}_4$  in this geologic area of carbonate rock and sediments is from siliceous periphyton (diatoms) growing in the Shark River Slough, Taylor Slough, and C-111 basin watersheds. Unlike the Mississippi River plume with CHLA concentrations of  $76 \mu\text{g l}^{-1}$  (Nelson and Dortch 1996), phytoplankton biomass on the Shelf ( $1\text{-}2 \mu\text{g l}^{-1}$  CHLA) was not sufficient to account for the depletion of  $\text{Si(OH)}_4$  in this area. Therefore,  $\text{Si(OH)}_4$  concentrations on the Shelf were depleted by mixing alone allowing  $\text{Si(OH)}_4$  to be used as a semi-conservative tracer of freshwater in this system (Ryther et al. 1967; Moore et al. 1986). Unlike Florida Bay and the west coast, there was very little  $\text{Si(OH)}_4$  loading to southern Biscayne Bay, mostly because the source of freshwater to this system is from canals which drain agricultural and urban areas of Dade County.

In the Lower and Middle Keys, it is clear that the source of  $\text{Si(OH)}_4$  to the nearshore Atlantic waters is through the Sluiceway and Backcountry (Fig. 11).  $\text{Si(OH)}_4$  concentrations near the

coast were elevated relative to the reef tract with much higher concentrations occurring in the Lower and Middle Keys than the Upper Keys. There is an interesting peak in  $\text{Si(OH)}_4$  concentration in an area of the Sluiceway which is densely covered with the seagrass, *Syringodium* (Fourqurean et al. 2002). We are unsure as to the source but postulate that it may be due to benthic flux.

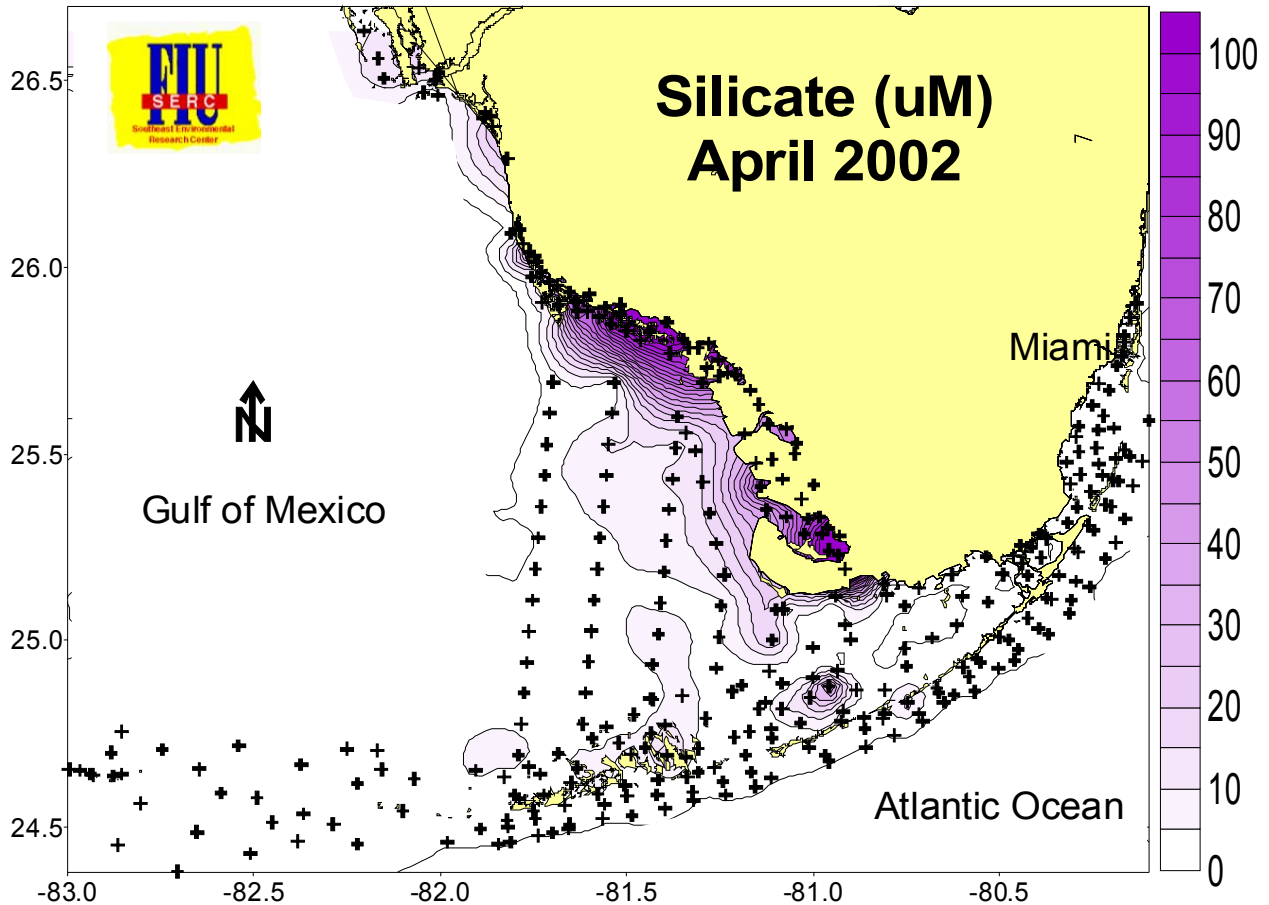


Figure 11. Example of silicate distributions across the region during spring 2002.

Visualization of spatial patterns of  $\text{NO}_3^-$  concentration over South Florida waters provide an extended view of source gradients over the region (Appendix). Biscayne Bay, Florida Bay, and the Shark River area of the west coast exhibited high  $\text{NO}_3^-$  concentrations relative to the FKNMS and Shelf. Elevated  $\text{NO}_3^-$  in Biscayne Bay is the result of loading from both the canal drainage system and from inshore groundwater (Alleman et al. 1995, Meeder et al. 1997). The source of  $\text{NO}_3^-$  to Florida Bay is the Taylor Slough and C-111 basin (Boyer and Jones, 1999; Rudnick et al., 1999) while the Shark River Slough impacts the west coast mangrove rivers and out onto the Shelf (Rudnick et al., 1999). We speculate that in both cases, elevated  $\text{NO}_3^-$  concentrations are

the result of  $N_2$  fixation/nitrification within the mangroves (Pelegrini and Twilley 1998). The oceanside transects off the uninhabited Upper Keys (off Biscayne Bay in Seg. 9) exhibited the lowest alongshore  $NO_3^-$  compared to the Middle and Lower Keys. A similar pattern was observed in a previous transect survey from these areas (Szmant and Forrester 1996). They also showed an inshore elevation of  $NO_3^-$  relative to Hawk Channel and the reef tract which is also demonstrated in our analysis (Fig. 12). Interestingly,  $NO_3^-$  concentrations in all stations in the Tortugas transect were similar to those of reef tract sites in the mainland Keys; there was no inshore elevation of  $NO_3^-$  on the transect off uninhabited Loggerhead Key. We suggest this source of  $NO_3^-$  in the Keys is due to human shoreline development.

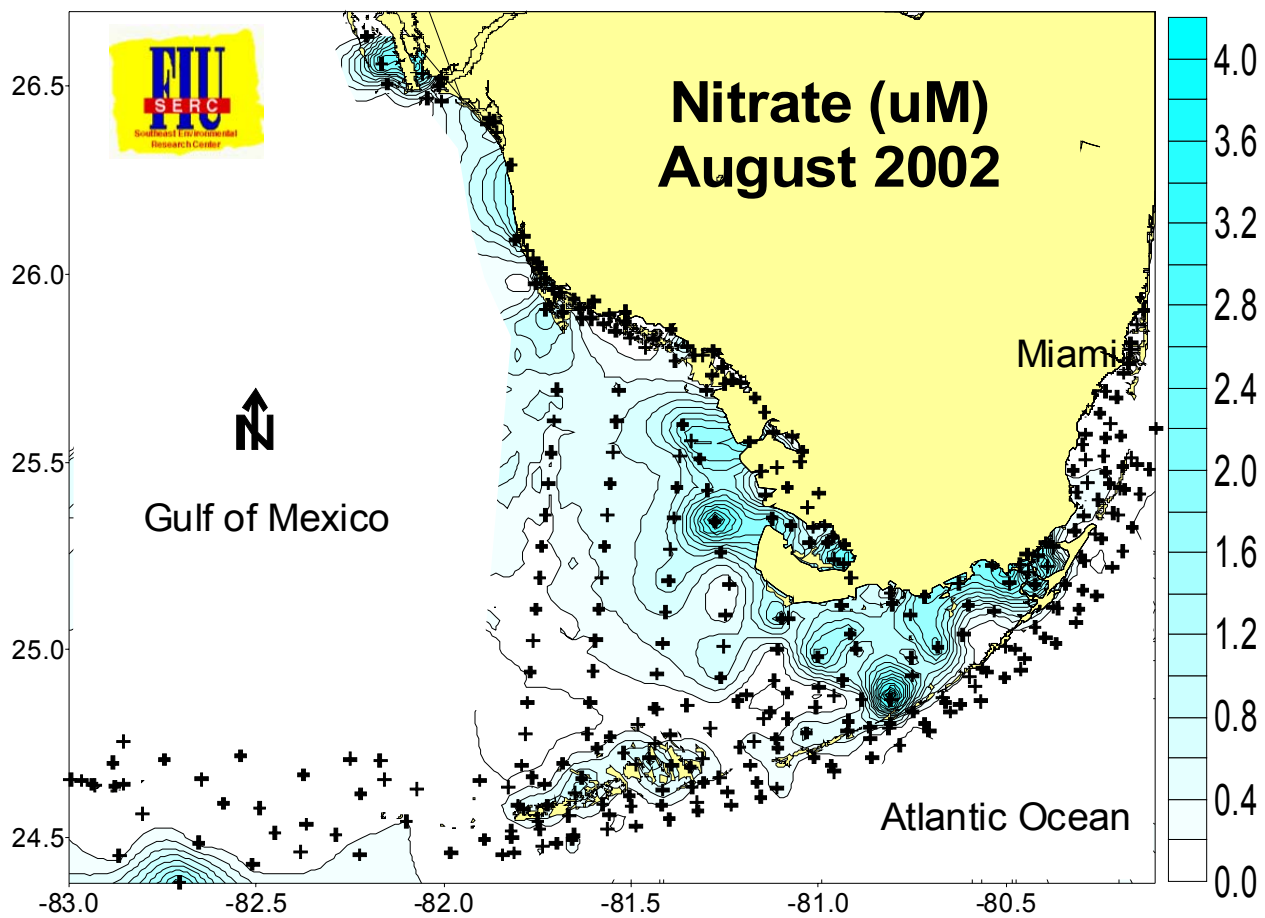


Figure 12. Example of nitrate distributions across the region during summer 2002.

Figure 12 also shows that a distinct intensification of  $NO_3^-$  occurs in the Backcountry region. Part of this increase may be due to local sources of  $NO_3^-$ , i.e. septic systems and stormwater runoff around Big Pine Key (Lapointe and Clark 1992). However, there is another area, the Snipe Keys, that also exhibits high  $NO_3^-$  which is uninhabited by man which rules out the



premise of septic systems being the only source of  $\text{NO}_3^-$  in this area. It is important to note that the Backcountry area is very shallow ( $\sim 0.5$  m) and hydraulically isolated from the Shelf and Atlantic which results in its having a relatively long water residence time. Elevated  $\text{NO}_3^-$  concentrations may be partially due to simple evaporative concentration as is seen in locally elevated salinity values. Another possibility is a contribution of benthic  $\text{N}_2$  fixation/nitrification in this very shallow area.

$\text{NH}_4^+$  concentrations were distributed in a similar manner as  $\text{NO}_3^-$  with highest levels occurring in Florida Bay, the Ten Thousand Islands, and the Backcountry.  $\text{NH}_4^+$  concentrations were very low in Biscayne Bay because it is not a major component of loading from the canal drainage system.  $\text{NH}_4^+$  also showed similarities with  $\text{NO}_3^-$  in its spatial distribution, being lowest in the Upper Keys and highest inshore relative to offshore. There was no alongshore elevation of  $\text{NH}_4^+$  concentrations in the Tortugas where levels were similar to those of reef tract sites in the mainland Keys. That the least developed portion of the Upper Keys in Biscayne National Park and uninhabited Loggerhead Key (Tortugas) exhibited lowest  $\text{NO}_3^-$  and  $\text{NH}_4^+$  concentrations is evidence of a local anthropogenic source for both of these variables along the ocean side of the Upper, Middle, and Lower Keys. This pattern of decline offshore implies an onshore N source which is diluted with distance from land by low nutrient Atlantic Ocean waters.

Elevated DIN concentrations in the Backcountry, on the other hand, are not so easily explained. We postulate that the high concentrations found there are due to a combination of anthropogenic loading, physical entrapment, and benthic  $\text{N}_2$  fixation. The relative contribution of these potential sources is unknown. Lapointe and Matzie (1996) have shown that stormwater and septic systems are responsible for increased DIN loading in and around Big Pine Key. The effect of increased water residence time in DIN concentration is probably small. Salinities in this area were only 1-2 higher than local seawater which resulted in a concentration effect of only 5-6%. Benthic  $\text{N}_2$  fixation may potentially be very important in the N budget of the Backcountry. Measured rates of  $\text{N}_2$  fixation in a *Thalassia* bed in Biscayne Bay, having very similar physical and chemical conditions, were  $540 \mu\text{mol N m}^{-2} \text{d}^{-1}$  (Capone and Taylor 1980). Without the plant community N demand, one day of  $\text{N}_2$  fixation has the potential to generate a water column concentration of  $>1 \mu\text{M NH}_4^+$  (0.5 m deep). Much of this  $\text{NH}_4^+$  is probably nitrified and may help account for the elevated  $\text{NO}_3^-$  concentrations observed in this area as well.

Clearly,  $N_2$  fixation may be a significant component of the N budget in the Backcountry and that it may be exported as DIN to the FKNMS in general.

Spatial patterns in TP in South Florida coastal waters were strongly driven by the west coast sources (Fig. 13). A small gradient in TP extended from the inshore waters of Whitewater Bay - Ten Thousand Islands mangrove complex out onto the Shelf and Tortugas. A weak gradient also extended from north central Florida Bay to the Middle Keys. Brand (1997) has postulated that groundwater from a subterranean Miocene quartz sand channel, "the river of sand", containing high levels of phosphorus is the source of TP in this region. However, little evidence of this source exists to date and field data from Florida Bay does not indicate a subterranean source (Corbett et al. 1999; Boyer and Jones unpublished data). Finally, there was no evidence of a significant terrestrial source of TP to Biscayne Bay.

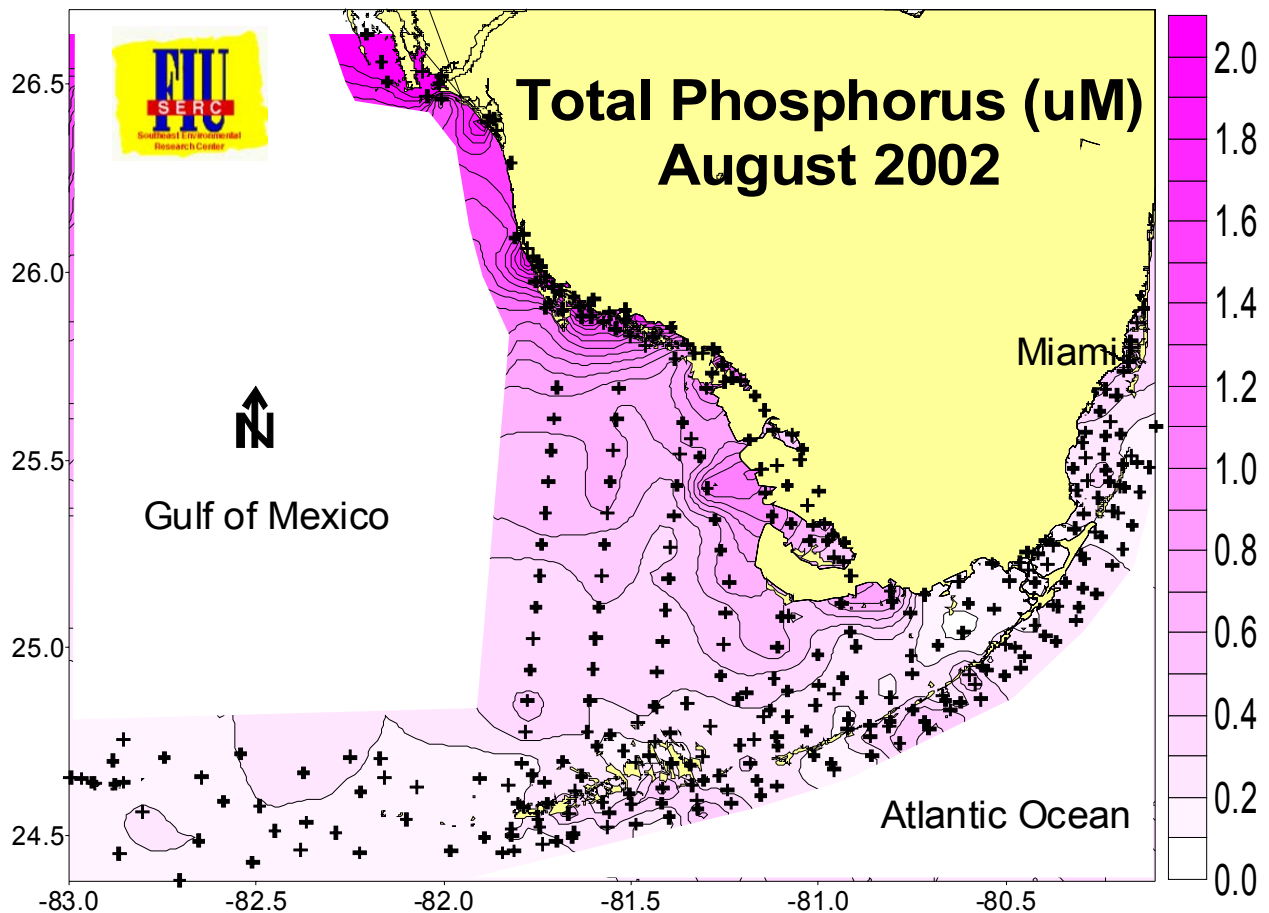


Figure 13. Example of total phosphorus distributions across the region during summer 2002.

In the Keys, there was evidence of elevated TP in alongshore stations of the Middle and Lower Keys but the differences were very small. The Upper Keys actually showed higher TP concentrations on the reef tract than inshore implying an offshore source. Interestingly, the

Tortugas area had higher TP concentrations than the Upper Keys as a result of Shelf water advection. In South Florida coastal waters, very little of TP is found in the inorganic form (SRP -  $\text{PO}_4^-$ ); most is organic P. The distribution of SRP on the west coast and Shelf was similar to that of TP with the general gradient from the west coast to Tortugas remaining (Appendix). However, the SRP distribution was distinctly different from that of TP in Florida Bay, Whitewater Bay, and Biscayne Bay. In central Florida Bay the N-S gradient previously observed for TP was highly diminished for SRP indicating that almost all the TP in central Florida Bay was in the form of organic P. It is unlikely that the source of TP to this region is from overland flow or groundwater as this is also the region that expresses highest salinity. Alternately, we hypothesize that the presence of the Flamingo channel, running parallel to the southern coastline of Cape Sable, acts as a tidal conduit for episodic advection of inshore Shelf water to enter north central Florida Bay. Subsequent trapping and evaporation then may act to concentrate TP in this region. The second difference in P distributions was that there was a significant SRP gradient present in NE Florida Bay that was not observed for TP. The sources of SRP to this area are the Taylor Slough and C-111 basin (W. Walker per. communication; Boyer and Jones, 1999; Rudnick et al., 1999). Whitewater Bay displayed an east-west gradient in SRP concentrations which increased with salinity leading us to conclude that the freshwater inputs from the Everglades were not a source of SRP to this area. Finally, there was evidence of a significant onshore-offshore SRP gradient in southern Biscayne Bay; most probably as a direct result of canal loading and groundwater seepage to this region (A. Lietz personal communication; Meeder et al. 1997).

Concentrations of TOC (Fig. 14) and TON (Appendix) are remarkably similar in pattern of distribution across the South Florida coastal hydroscape. The decreasing gradient from west coast to Tortugas was very similar to that of TP. A steep gradient with distance from land was also observed in Biscayne Bay. Both these gradients were most probably due to terrestrial loading. On the west coast, the source of TOC and TON was from the mangrove forests. Our data from this area shows that concentrations of TOC and TON increased from Everglades headwaters through the mangrove zone and then decrease with distance offshore. In Biscayne Bay, much of the TOC and TON is from agricultural land use. The high concentrations of TOC and TON found in Florida Bay were due to a combination of terrestrial loading (Boyer and

Jones, 1999), in situ production by seagrass and phytoplankton, and evaporative concentration (Fourqurean et al. 1993).

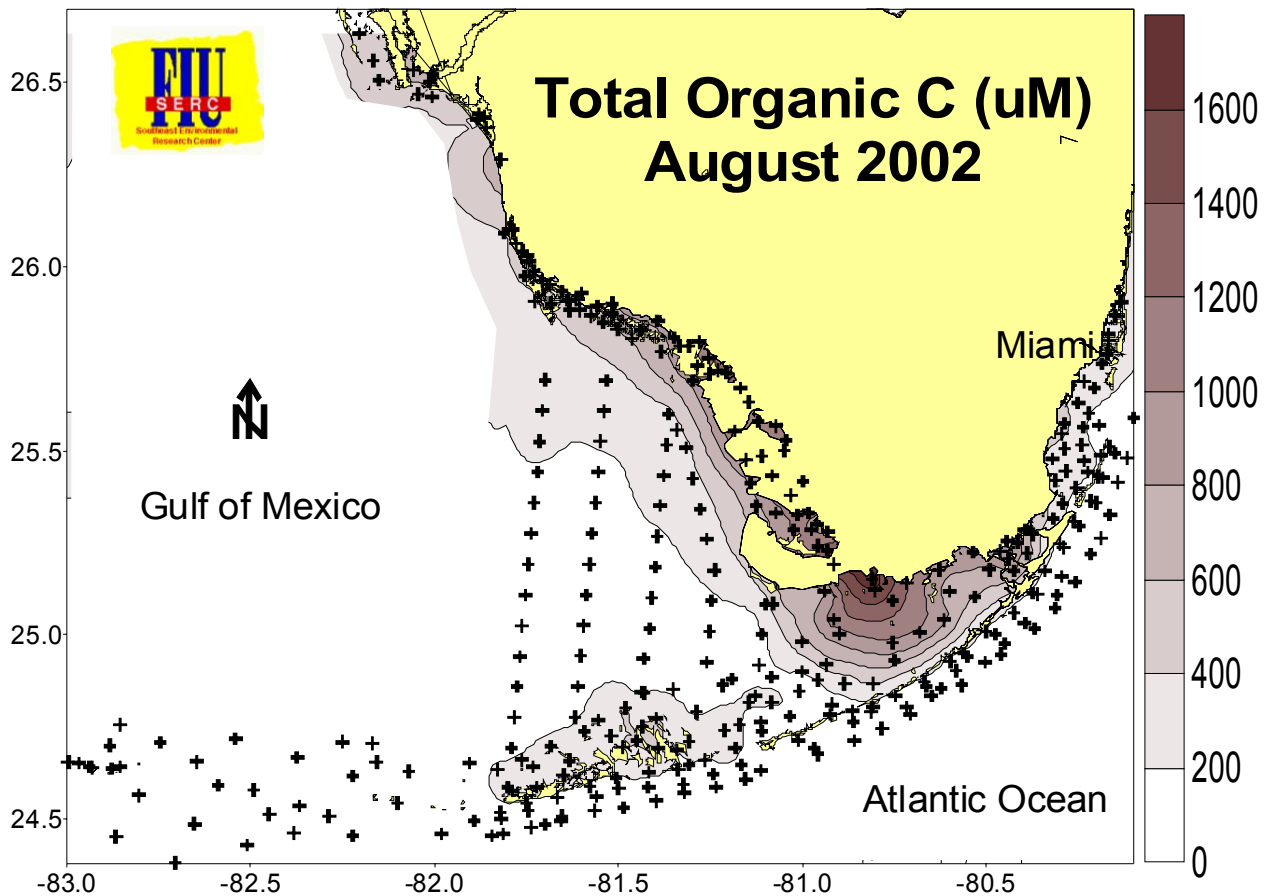


Figure 14. Example of total organic carbon distributions across the region during summer 2002.

Advection of Shelf and Florida Bay waters through the Sluiceway and passes accounted for this region and the inshore area of the Middle Keys as having highest TOC and TON of the FKNMS. Strong offshore gradients in TOC and TON existed for all mainland Keys segments but not for the Tortugas transect. Part of this difference may be explained by the absence of mangroves in the single Tortugas transect. The higher concentrations of TOC and TON in the inshore waters of the Keys implies a terrestrial source rather than simply benthic production and sediment resuspension. Main Keys reef tract concentrations of TOC and TON were similar to those found in the Tortugas.

Much emphasis has been placed on assessing the impact of episodic phytoplankton blooms in Florida Bay on the offshore reef tract environment. Spatial patterns of CHLA concentrations showed that NW Florida Bay, Whitewater Bay, and the Ten Thousand Islands exhibited high

levels of CHLA relative to Biscayne Bay, Shelf, and FKNMS (Fig. 15). The highest CHLA concentrations were found in west coast mangrove estuaries (up to  $45 \mu\text{g l}^{-1}$  in Alligator Bay, TTI). CHLA is also routinely higher ( $\sim 2 \mu\text{g l}^{-1}$ ) in NW Florida Bay along the channel connecting the Shelf to Flamingo. It is interesting that CHLA concentrations are higher in the Marquesas ( $0.36 \mu\text{g l}^{-1}$ ) than in other areas of the FKNMS. When examined in context with the whole South Florida ecosystem, it is obvious that the Marquesas zone should be considered a continuum of the Shelf rather than a separate management entity. This shallow sandy area (often called the Quicksands) acts as a physical mixing zone between the Shelf and the Atlantic Ocean and is a highly productive area for other biota as well as it encompasses the historically rich Tortugas shrimping grounds. A CHLA concentration of  $2 \mu\text{g l}^{-1}$  in the water column of a reef tract might be considered an indication of eutrophication. Conversely, a similar CHLA level in the Quicksands indicates a productive ecosystem which feeds a valuable shrimp fishery.

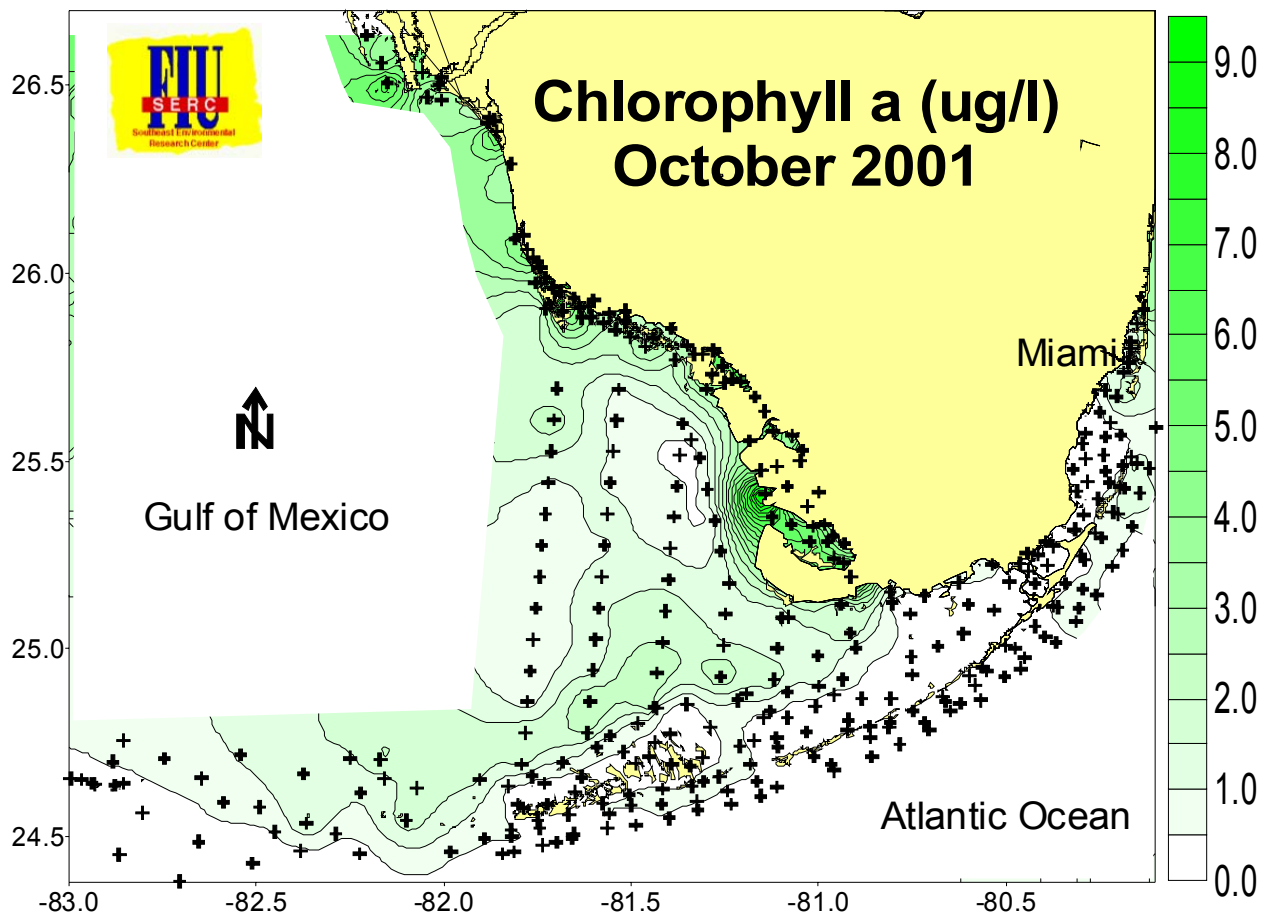


Figure 15. Example of chlorophyll a distributions across the region during fall 2001.

The oceanside transects in the Upper Keys exhibited the lowest overall CHLA concentrations of any zone in the FKNMS. Transects off the Middle and Lower Keys showed that a drop in CHLA occurred at reef tract sites; there was no linear decline with distance from shore. Interestingly, CHLA concentrations in the Tortugas transect showed a similar pattern as the mainland Keys. Inshore and Hawk Channel CHLA concentrations among Middle Keys, Lower Keys and Tortugas sites were not significantly different. As inshore CHLA concentrations in the Tortugas were similar to those in the Middle and Lower Keys, we see no evidence of persistent phytoplankton bloom transport from Florida Bay.

Along with TP concentration, turbidity is probably the second most important determinant of local ecosystem health (Fig. 16). The fine grained, low density carbonate sediments in this area are easily resuspended, rapidly transported, and have high light scattering potential. Sustained high turbidity of the water column indirectly affects benthic community structure by decreasing light penetration, promoting seagrass extinction.

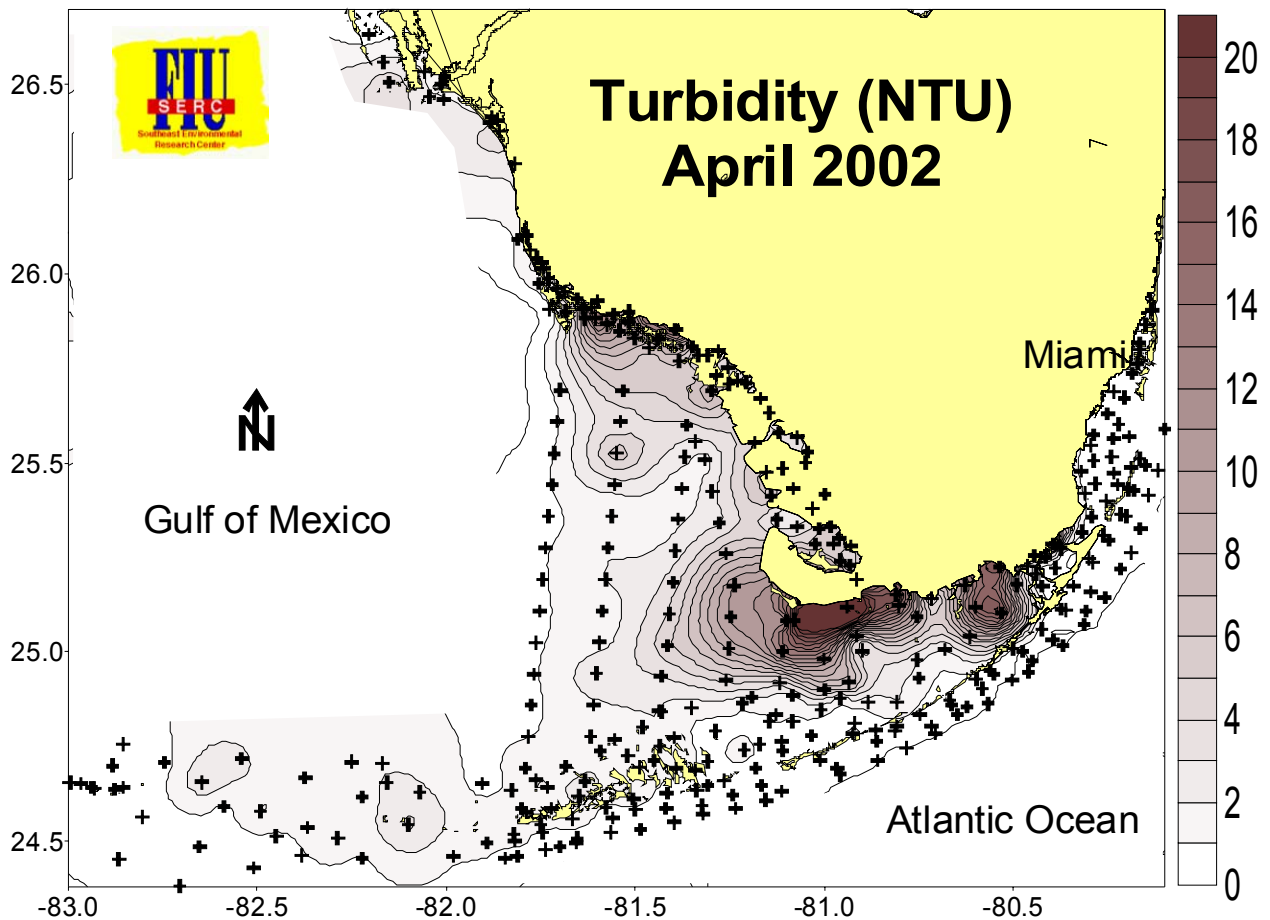


Figure 16. Example of turbidity distributions across the region during spring 2002.

Large scale observations of turbidity clearly show patterns of onshore-offshore gradients which extend out onto the Shelf to the Marquesas (Appendix; Stumpf et al. 1999). In the last seven years, turbidities in Florida Bay have increased dramatically in the NE and central regions (Boyer et al. 1998) potentially as a consequence of destabilization of the sediment from seagrass die-off (Robblee et al. 1991). Strong turbidity gradients were observed for all Keys transects but reef tract levels were remarkably similar regardless of inshore levels. High alongshore turbidity is most probably due to the shallow water column being easily resuspended by wind and wave action. Light extinction ( $K_d$ ) was highest alongshore and improved with distance from land. This trend was expected as light extinction is directly related to water turbidity.

Using the TN:TP ratio is a relatively simple method of estimating potential nutrient limitation status of phytoplankton (Redfield 1967). Most of the South Florida hydroscape was shown to have TN:TP values  $\gg 16:1$ , indicating the potential for phytoplankton to be limited by P at these sites (Fig. 17).

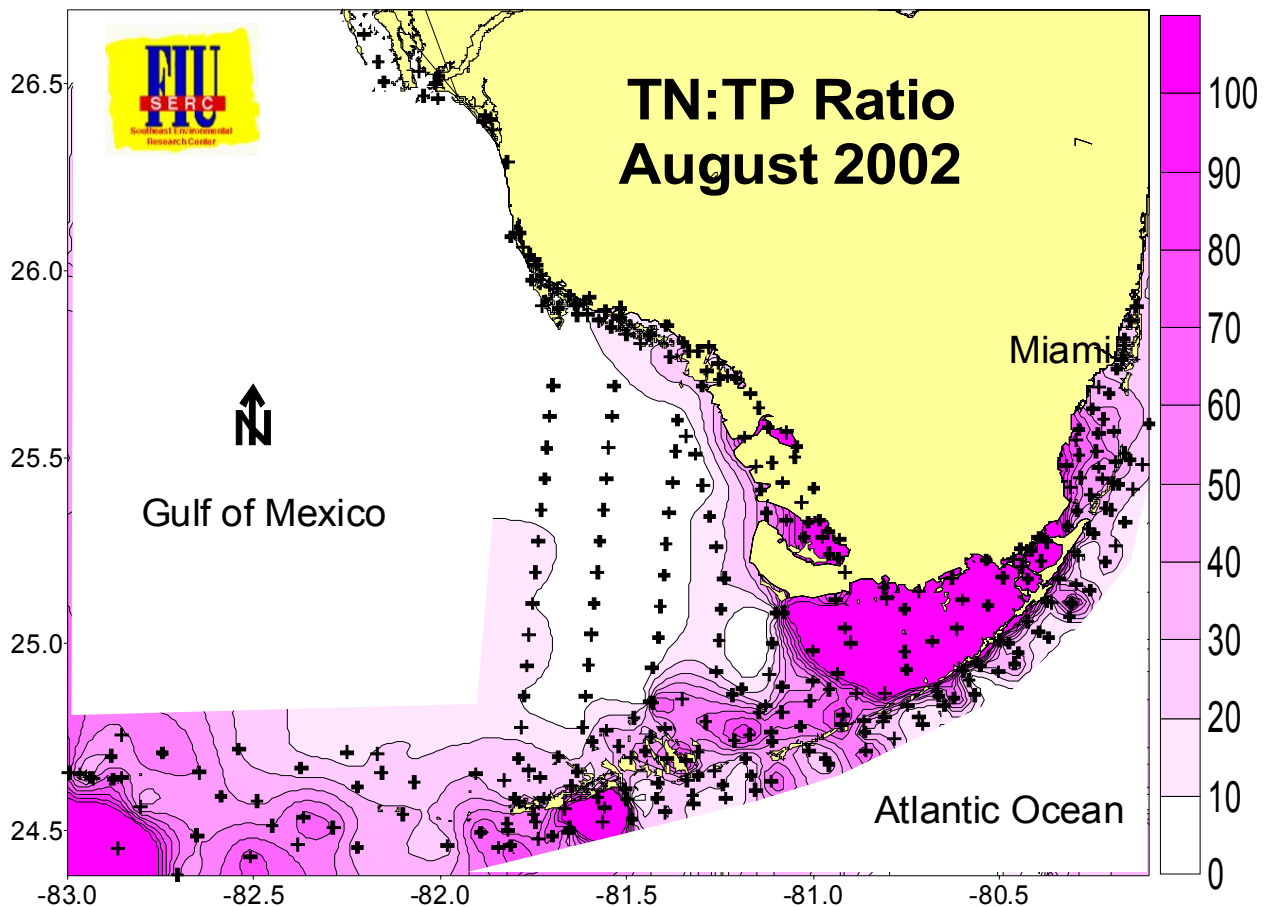


Figure 17. Example of TN:TP ratio distribution across the region during summer 2002.

The bulk of Florida Bay and both southern and northern Biscayne Bay were severely P limited, mostly as a result of high DIN concentrations. All of the FKNMS is routinely P limited using this metric. Interestingly, the Marquesas/Quicksands area was the least P limited of all zones and exhibited a significant regression between SRP and CHLA. Only in the northern Ten Thousand Islands and Shelf did N become the limiting nutrient. The south-north shift from P to N limitation observed in the west coast estuaries has been ascribed to changes in landuse and bedrock geochemistry of the watersheds (Boyer and Jones 1998). The west coast south of 25.4 N latitude is influenced by overland freshwater flow from the Everglades and Shark River Slough having very low P concentrations relative to N. Above 25.7 N latitude the bedrock geology of the watershed changes from carbonate to silicate based and landuse changes from relatively undeveloped wetland (Big Cypress Basin) to a highly urban/agricultural mix (Naples, FL).

Temporal trends in water quality showed most variables to be relatively consistent from year to year, with some showing seasonal excursions. The exception was the increasing variability in TP concentrations throughout the region. This brings up an important point that, when looking at what are perceived to be local trends, we find that they seem to occur across the whole region but at more damped amplitudes. This spatial autocorrelation in water quality is an inherent property of highly interconnected systems such as coastal and estuarine ecosystems driven by similar hydrological and climatological forcings. Clearly, there have been large changes in the FKNMS water quality over time, but no sustained monotonic trends have been observed. We must always keep in mind that trend analysis is limited to the window of observation; trends may change with additional data collection.

The large scale of this monitoring program has allowed us to assemble a much more holistic view of broad physical/chemical/biological interactions occurring over the South Florida hydroscape. Much information has been gained by inference from this type of data collection program: major nutrient sources have been confirmed, relative differences in geographical determinants of water quality have been demonstrated, and large scale transport via circulation pathways have been elucidated. In addition we have shown the importance of looking "outside the box" for questions asked within. Rather than thinking of water quality monitoring as being a static, non-scientific pursuit it should be viewed as a tool for answering management questions and developing new scientific hypotheses.



We continue to maintain a website (<http://serc.fiu.edu/wqmnetwork/>) where data from the FKNMS is integrated with the other parts of the SERC water quality network (Florida Bay, Whitewater Bay, Biscayne Bay, Ten Thousand Islands, and SW Florida Shelf) and displayed as downloadable contour maps, time series graphs, and interpretive reports.

### Acknowledgments

We thank all the field and laboratory technicians involved with this project, especially Sean Murray, John Fulop, and Pete Lorenzo. We also thank the captains and crew of the R/V Bellows of the Florida Institute of Oceanography for their professional support of the monitoring program. This project was possible due to continued funding by the US-EPA (Agreement #X994621-94-0), the South Florida Water Management District (Contract #C-13178), and the Monroe County Tourist Development Council. This is Technical Report #T192 of the Southeast Environmental Research Center at Florida International University.

## V. References

- ALLEMAN, R. W., ET AL. 1995. Biscayne Bay surface water improvement and management. Technical supporting document. South Florida Water Management District.
- BOYER, J. N., J. W. FOURQUREAN, AND R. D. JONES. 1997. Spatial characterization of water quality in Florida Bay and Whitewater Bay by multivariate analysis: Zones of similar influence (ZSI). Estuaries 20: 743-758.
- BOYER, J. N., J. W. FOURQUREAN, AND R. D. JONES. 1999. Seasonal and long term trends in the water quality of Florida Bay (1989 - 1997). Estuaries 22: 417-430.
- BOYER, J. N., AND R. D. JONES. 1998. Influence of coastal morphology and watershed characteristics on the water quality of mangrove estuaries in the Ten Thousand Islands - Whitewater Bay complex. Proceedings of the 1998 Florida Bay Science Conference. University of Florida Sea Grant.
- BOYER, J. N., AND R. D. JONES. 1999. Effects of freshwater inputs and loading of phosphorus and nitrogen on the water quality of Eastern Florida Bay, p. 545-561. *In* K. R. Reddy, G. A. O'Connor, and C. L. Schelske (eds.) Phosphorus biogeochemistry in sub-tropical ecosystems. CRC/Lewis Publishers, Boca Raton, Florida.
- BOYER, J. N., AND R. D. JONES. 2002. A view from the bridge: External and internal forces affecting the ambient water quality of the Florida Keys National Marine Sanctuary, p. 609-628. *In* J. W. Porter and K. G. Porter (eds.), The Everglades, Florida Bay, and Coral Reefs of the Florida Keys: An Ecosystem Sourcebook. CRC Press.
- BOYER, J. N., P. STERLING, AND R. D. JONES. 2000. Maximizing information from a water quality monitoring network through visualization techniques. Estuarine, Coastal and Shelf Science 50: 39-48.
- BRAND, L. 1998. The role of groundwater in the Florida Bay ecosystem. Proceedings of the 1998 Florida Bay Science Conference. University of Florida Sea Grant.
- CAPONE, D. G., AND B. F. TAYLOR. 1980. Microbial nitrogen cycling in a seagrass community, p. 153-161. *In* V. S. Kennedy (ed.), Estuarine Perspectives. Academic.
- CHRISTIAN, R. R., J. N. BOYER, D. W. STANLEY, AND W. M. RIZZO. 1991. Multi-year distribution patterns of nutrients in the Neuse River Estuary, North Carolina. Marine Ecology Progress Series 71:259-274.

- ENVIRONMENTAL PROTECTION AGENCY. 1995. Water quality protection program for the Florida Keys National Marine Sanctuary: Phase III report. Final report submitted to the Environmental Protection Agency under Work Assignment 1, Contract No. 68-C2-0134. Battelle Ocean Sciences, Duxbury, MA and Continental Shelf Associates, Inc., Jupiter FL.
- FOURQUREAN, J.W., M.D. DURAKO, M.O. HALL AND L.N. HEFTY. 2002. Seagrass distribution in south Florida: a multi-agency coordinated monitoring program, p. 497-522. *In* J. W. Porter and K. G. Porter (eds.), *The Everglades, Florida Bay, and Coral Reefs of the Florida Keys: An Ecosystem Sourcebook*. CRC Press.
- HIRSCH, R. M., R. B. ALEXANDER, AND R. A. SMITH. 1991. Selection of methods for the detection and estimation of trends in water quality. *Water Resources Research* 27:803-813.
- ISAAKS, E. H., AND R. M. SRIVASTAVA. 1989. *An Introduction to Applied Geostatistics*. Oxford Press, 561 pp.
- JONES, R. D., AND J. N. BOYER 2001. 2000 Annual Report of the Water Quality Monitoring Project for the Florida Keys National Marine Sanctuary. SERC Technical Report #T151.
- KLEIN, C. J., AND S. P. ORLANDO JR. 1994. A spatial framework for water-quality management in the Florida Keys National Marine Sanctuary. *Bulletin of Marine Science* 54: 1036-1044.
- LAPOINTE, B. E., AND M. W. CLARK. 1992. Nutrient inputs from the watershed and coastal eutrophication in the Florida Keys. *Estuaries* 15: 465-476.
- LAPOINTE, B. E., AND W. R. MATZIE. 1996. Effects of stormwater nutrient discharges on eutrophication processes in nearshore waters of the Florida Keys. *Estuaries* 19: 422-435.
- LEE, T. N., M. E. CLARKE, E. WILLIAMS, A. F. SZMANT, AND T. BERGER. 1994. Evolution of the Tortugas gyre and its influence on recruitment in the Florida Keys. *Bulletin of Marine Science* 54: 621-646.
- LEE, T. N., E. WILLIAMS, E. JOHNS, D. WILSON, AND N. P. SMITH. 2002. Transport processes linking South Florida ecosystems, p. 309-342. *In* J. W. Porter and K. G. Porter (eds.), *The Everglades, Florida Bay, and Coral Reefs of the Florida Keys: An Ecosystem Sourcebook*. CRC Press.
- LEICHTER, J. J., S. R. WING, S. L. MILLER, AND M. W. DENNY. 1996. Pulsed delivery of subthermocline water to Conch Reef (Florida Keys) by internal tidal bores. *Limnology and Oceanography* 41: 1490-1501.

- LEICHTER, J. J., AND S. L. MILLER. 1999. Predicting high-frequency upwelling: Spatial and temporal patterns of temperature anomalies on a Florida coral reef. Continental Shelf Research 19: 911-928
- MEEDER, J. F., J. ALVORD, M. BYRNE, M. S. ROSS, AND A. RENSHAW. 1997. Distribution of benthic nearshore communities and their relationship to groundwater nutrient loading. Final report to Biscayne National Park.
- MOORE, W. S., J. L. SARMIENTO, AND R. M. KEY. 1986. Tracing the Amazon component of surface Atlantic water using  $^{228}\text{Ra}$ , salinity, and silica. Journal of Geophysical Research 91: 2574-2580.
- NELSON, D. M., AND Q. DORTCH. 1996. Silicic acid depletion and silicon limitation in the plume of the Mississippi River: evidence from kinetic studies in spring and summer. Marine Ecology Progress Series 136: 163-178.
- NATIONAL OCEANIC AND ATMOSPHERIC ADMINISTRATION. 1995. Florida Keys National Marine Sanctuary Draft Management Plan/Environmental Impact Statement.
- OVERLAND, J. E. AND R. W. PREISENDORFER. 1982. A significance test for principal components applied to cyclone climatology. Monthly Weather Review 110:1-4.
- PITTS, P. A. 1997. An investigation of tidal and nontidal current patterns in Western Hawk Channel, Florida Keys. Continental Shelf Research 17: 1679-1687.
- REDFIELD, A. C. 1958. The biological control of chemical factors in the environment. American Scientist 46: 205-222.
- ROBBLEE, M. B., T. B. BARBER, P. R. CARLSON JR., M. J. DURAKO, J. W. FOURQUREAN, L. M. MUEHLSTEIN, D. PORTER, L. A. YABRO, R. T. ZIEMAN, AND J. C. ZIEMAN. 1991. Mass mortality of the tropical seagrass *Thalassia testudinum* in Florida Bay (USA). Marine Ecology Progress Series 71: 297-299.
- RUDNICK, D., Z. CHEN, D. CHILDERS, T. FONTAINE, AND J. N. BOYER. 1999. Phosphorus and nitrogen inputs to Florida Bay: the importance of the Everglades watershed. Estuaries 22: 398-416.
- RYTHER, J. H., D. W. MENZE, AND N. CORWIN. 1967. Influence of the Amazon River outflow on the ecology of the western tropical Atlantic, I. Hydrography and nutrient chemistry. Journal of Marine Research 25: 69-83.

- SMITH, N. P. 1994. Long-term Gulf-to-Atlantic transport through tidal channels in the Florida Keys. Bulletin of Marine Science 54: 602-609.
- STUMPF, R. P., M. L. FRAYER, M. J. DURAKO, AND J. C. BROCK. 1999. Variations in water clarity and bottom albedo in Florida Bay from 1985-1997. Estuaries 22: 431-444.
- SZMANT, A. M., AND A. FORRESTER. 1996. Water column and sediment nitrogen and phosphorus distribution patterns in the Florida Keys, USA. Coral Reefs 15: 21-41.

## **VI. Appendices**

### **Appendix 1**

Color contour maps of water quality variables by sampling event may be viewed and downloaded at <http://serc.fiu.edu/wqmnetwork/CONTOUR%20MAPS/ContourMaps.htm>.

These maps encompass all 354 stations of the SERC Water Quality Monitoring Network which includes the FKNMS, Biscayne Bay, Florida Bay, Whitewater Bay, Ten Thousand Islands, and Southwest Florida Shelf. The data was collected over a period of a month so care should be taken in interpreting these maps as they are not truly synoptic.

## Appendix 2

**Table 3.** Statistical summary of water quality in zones for the period of record. Data are summarized as median, minimum (Min.), maximum value (Max.), and number of samples (*n*).

| <b>Variable</b>                      | <b>Cluster</b> | <b>Median</b> | <b>Min.</b> | <b>Max.</b> | <b><i>n</i></b> |
|--------------------------------------|----------------|---------------|-------------|-------------|-----------------|
| Surface                              | 1              | 0.10          | 0.00        | 2.18        | 404             |
| NO <sub>3</sub> <sup>-</sup><br>(μM) | 2              | 0.09          | 0.00        | 1.24        | 56              |
|                                      | 3              | 0.06          | 0.00        | 2.30        | 1727            |
|                                      | 4              | 0.04          | 0.00        | 0.76        | 144             |
|                                      | 5              | 0.19          | 0.00        | 2.11        | 562             |
|                                      | 6              | 0.08          | 0.00        | 5.90        | 832             |
|                                      | 7              | 0.33          | 0.00        | 4.42        | 316             |
|                                      | 8              | 0.06          | 0.00        | 2.11        | 345             |
|                                      | Bottom         | 1             | 0.04        | 0.00        | 1.33            |
| NO <sub>3</sub> <sup>-</sup><br>(μM) | 2              |               |             |             |                 |
|                                      | 3              | 0.08          | 0.00        | 4.46        | 1622            |
|                                      | 4              |               |             |             |                 |
|                                      | 5              | 0.12          | 0.00        | 1.17        | 97              |
|                                      | 6              | 0.09          | 0.00        | 5.01        | 693             |
|                                      | 7              | 0.06          | 0.01        | 0.39        | 3               |
|                                      | 8              | 0.07          | 0.00        | 1.94        | 230             |
|                                      | Surface        | 1             | 0.05        | 0.00        | 0.35            |
| NO <sub>2</sub> <sup>-</sup><br>(μM) | 2              | 0.06          | 0.00        | 0.24        | 56              |
|                                      | 3              | 0.03          | 0.00        | 0.71        | 1734            |
|                                      | 4              | 0.05          | 0.00        | 0.22        | 144             |
|                                      | 5              | 0.06          | 0.00        | 0.25        | 564             |
|                                      | 6              | 0.04          | 0.00        | 0.42        | 833             |
|                                      | 7              | 0.09          | 0.00        | 0.40        | 316             |
|                                      | 8              | 0.04          | 0.00        | 0.34        | 345             |
|                                      | Bottom         | 1             | 0.04        | 0.02        | 0.17            |
| NO <sub>2</sub> <sup>-</sup><br>(μM) | 2              |               |             |             |                 |
|                                      | 3              | 0.04          | 0.00        | 1.73        | 1627            |
|                                      | 4              |               |             |             |                 |
|                                      | 5              | 0.06          | 0.00        | 0.18        | 98              |
|                                      | 6              | 0.04          | 0.00        | 0.36        | 693             |
|                                      | 7              | 0.06          | 0.04        | 0.10        | 4               |
|                                      | 8              | 0.05          | 0.00        | 0.32        | 230             |

| <b>Variable</b>                      | <b>Cluster</b> | <b>Median</b> | <b>Min.</b> | <b>Max.</b> | <b><i>n</i></b> |
|--------------------------------------|----------------|---------------|-------------|-------------|-----------------|
| Surface                              | 1              | 0.41          | 0.00        | 1.84        | 403             |
| NH <sub>4</sub> <sup>+</sup><br>(μM) | 2              | 0.39          | 0.08        | 10.32       | 56              |
|                                      | 3              | 0.24          | 0.00        | 2.30        | 1734            |
|                                      | 4              | 0.28          | 0.00        | 2.22        | 144             |
|                                      | 5              | 0.38          | 0.00        | 4.03        | 564             |
|                                      | 6              | 0.27          | 0.00        | 5.03        | 833             |
|                                      | 7              | 0.56          | 0.00        | 4.62        | 316             |
|                                      | 8              | 0.28          | 0.00        | 2.21        | 345             |
|                                      | Bottom         | 1             | 0.28        | 0.00        | 0.95            |
| NH <sub>4</sub> <sup>+</sup><br>(μM) | 2              |               |             |             |                 |
|                                      | 3              | 0.25          | 0.00        | 2.90        | 1625            |
|                                      | 4              |               |             |             |                 |
|                                      | 5              | 0.36          | 0.04        | 1.52        | 98              |
|                                      | 6              | 0.29          | 0.00        | 3.88        | 693             |
|                                      | 7              | 0.44          | 0.30        | 0.64        | 4               |
|                                      | 8              | 0.29          | 0.00        | 1.26        | 230             |
|                                      | Surface        | 1             | 15.08       | 2.46        | 71.94           |
| TN<br>(μM)                           | 2              | 14.92         | 3.90        | 63.44       | 56              |
|                                      | 3              | 8.61          | 1.71        | 67.85       | 1731            |
|                                      | 4              | 15.10         | 4.22        | 69.95       | 144             |
|                                      | 5              | 14.11         | 2.27        | 86.60       | 562             |
|                                      | 6              | 10.34         | 1.81        | 211.10      | 831             |
|                                      | 7              | 16.50         | 2.54        | 73.72       | 317             |
|                                      | 8              | 11.15         | 2.18        | 70.17       | 345             |
|                                      | Bottom         | 1             | 10.65       | 2.47        | 32.62           |
| TN<br>(μM)                           | 2              |               |             |             |                 |
|                                      | 3              | 8.27          | 1.48        | 52.66       | 1624            |
|                                      | 4              |               |             |             |                 |
|                                      | 5              | 13.72         | 3.01        | 52.83       | 93              |
|                                      | 6              | 10.39         | 2.37        | 152.23      | 681             |
|                                      | 7              | 17.78         | 15.53       | 21.80       | 3               |
|                                      | 8              | 9.85          | 2.30        | 29.39       | 230             |
|                                      | Surface        | 1             | 14.43       | 1.97        | 71.65           |
| TON<br>(μM)                          | 2              | 14.08         | 3.41        | 62.91       | 56              |
|                                      | 3              | 8.10          | 0.89        | 67.72       | 1722            |
|                                      | 4              | 14.67         | 3.03        | 69.19       | 144             |
|                                      | 5              | 13.23         | 1.78        | 85.88       | 558             |
|                                      | 6              | 9.84          | 0.39        | 210.78      | 828             |
|                                      | 7              | 15.44         | 1.79        | 73.23       | 316             |
|                                      | 8              | 10.73         | 1.55        | 70.00       | 345             |



| <b>Variable</b>                     | <b>Cluster</b> | <b>Median</b> | <b>Min.</b> | <b>Max.</b> | <b><i>n</i></b> |
|-------------------------------------|----------------|---------------|-------------|-------------|-----------------|
| Bottom<br>TON<br>( $\mu\text{M}$ )  | 1              | 10.33         | 2.21        | 30.89       | 30              |
|                                     | 2              |               |             |             |                 |
|                                     | 3              | 7.72          | 0.00        | 51.94       | 1611            |
|                                     | 4              |               |             |             |                 |
|                                     | 5              | 13.10         | 2.47        | 52.67       | 93              |
|                                     | 6              | 9.76          | 0.00        | 151.91      | 676             |
|                                     | 7              | 15.91         | 15.14       | 16.68       | 2               |
|                                     | 8              | 9.49          | 1.90        | 27.80       | 229             |
| Surface<br>TP<br>( $\mu\text{M}$ )  | 1              | 0.27          | 0.09        | 1.09        | 403             |
|                                     | 2              | 0.25          | 0.12        | 0.83        | 56              |
|                                     | 3              | 0.18          | 0.00        | 1.22        | 1732            |
|                                     | 4              | 0.24          | 0.07        | 0.46        | 144             |
|                                     | 5              | 0.20          | 0.02        | 1.39        | 565             |
|                                     | 6              | 0.18          | 0.00        | 1.78        | 834             |
|                                     | 7              | 0.21          | 0.03        | 0.84        | 317             |
|                                     | 8              | 0.26          | 0.08        | 1.35        | 343             |
| Bottom<br>TP<br>( $\mu\text{M}$ )   | 1              | 0.21          | 0.13        | 0.45        | 29              |
|                                     | 2              |               |             |             |                 |
|                                     | 3              | 0.18          | 0.00        | 1.50        | 1622            |
|                                     | 4              |               |             |             |                 |
|                                     | 5              | 0.19          | 0.02        | 0.61        | 93              |
|                                     | 6              | 0.18          | 0.00        | 0.76        | 687             |
|                                     | 7              | 0.18          | 0.14        | 0.39        | 3               |
|                                     | 8              | 0.24          | 0.10        | 0.67        | 229             |
| Surface<br>SRP<br>( $\mu\text{M}$ ) | 1              | 0.02          | 0.00        | 0.30        | 404             |
|                                     | 2              | 0.02          | 0.00        | 0.22        | 56              |
|                                     | 3              | 0.01          | 0.00        | 0.23        | 1724            |
|                                     | 4              | 0.01          | 0.00        | 0.26        | 144             |
|                                     | 5              | 0.01          | 0.00        | 0.23        | 562             |
|                                     | 6              | 0.01          | 0.00        | 0.21        | 832             |
|                                     | 7              | 0.01          | 0.00        | 0.20        | 316             |
|                                     | 8              | 0.02          | 0.00        | 0.20        | 345             |
| Bottom<br>SRP<br>( $\mu\text{M}$ )  | 1              | 0.01          | 0.00        | 0.17        | 30              |
|                                     | 2              |               |             |             |                 |
|                                     | 3              | 0.01          | 0.00        | 0.39        | 1620            |
|                                     | 4              |               |             |             |                 |
|                                     | 5              | 0.01          | 0.00        | 0.10        | 98              |
|                                     | 6              | 0.01          | 0.00        | 0.36        | 691             |
|                                     | 7              | 0.01          | 0.01        | 0.11        | 5               |
|                                     | 8              | 0.02          | 0.00        | 0.14        | 230             |

| <b>Variable</b>                                   | <b>Cluster</b> | <b>Median</b> | <b>Min.</b> | <b>Max.</b> | <b><i>n</i></b> |
|---|----------------|---------------|-------------|-------------|-----------------|
| Surface<br>APA<br>( $\mu\text{M hr}^{-1}$ )       | 1              | 0.09          | 0.01        | 5.62        | 401             |
|   | 2              | 0.08          | 0.02        | 0.55        | 56              |
|   | 3              | 0.04          | 0.01        | 0.79        | 1617            |
|   | 4              | 0.08          | 0.03        | 0.52        | 144             |
|   | 5              | 0.07          | 0.01        | 2.52        | 559             |
|   | 6              | 0.06          | 0.00        | 0.45        | 823             |
|   | 7              | 0.10          | 0.03        | 1.43        | 317             |
|   | 8              | 0.06          | 0.02        | 3.03        | 315             |
| Bottom<br>APA<br>( $\mu\text{M hr}^{-1}$ )        | 1              | 0.06          | 0.02        | 0.46        | 26              |
|   | 2              |               |             |             |                 |
|   | 3              | 0.04          | 0.00        | 0.38        | 1508            |
|   | 4              |               |             |             |                 |
|   | 5              | 0.07          | 0.00        | 0.49        | 96              |
|   | 6              | 0.06          | 0.01        | 0.43        | 687             |
|   | 7              | 0.05          | 0.05        | 0.05        | 2               |
|   | 8              | 0.05          | 0.02        | 0.34        | 201             |
| Surface<br>Chl <i>a</i><br>( $\text{mg l}^{-1}$ ) | 1              | 0.34          | 0.00        | 15.24       | 405             |
|   | 2              | 0.30          | 0.00        | 4.95        | 56              |
|   | 3              | 0.23          | 0.00        | 2.98        | 1730            |
|   | 4              | 0.24          | 0.00        | 7.35        | 143             |
|   | 5              | 0.24          | 0.00        | 2.79        | 565             |
|   | 6              | 0.25          | 0.00        | 1.45        | 834             |
|   | 7              | 0.23          | 0.00        | 6.20        | 316             |
|   | 8              | 0.49          | 0.00        | 6.81        | 345             |
| Surface<br>TOC<br>( $\mu\text{M}$ )               | 1              | 246.8         | 124.3       | 1435.4      | 405             |
|   | 2              | 255.9         | 149.7       | 505.5       | 56              |
|   | 3              | 166.4         | 87.0        | 1054.8      | 1731            |
|   | 4              | 256.7         | 150.9       | 702.5       | 144             |
|   | 5              | 229.8         | 118.0       | 670.3       | 564             |
|   | 6              | 185.4         | 83.8        | 805.3       | 831             |
|   | 7              | 260.8         | 105.2       | 1653.5      | 317             |
|   | 8              | 205.0         | 102.8       | 950.4       | 345             |
| Bottom<br>TOC<br>( $\mu\text{M}$ )                | 1              | 205.1         | 121.4       | 446.0       | 30              |
|   | 2              |               |             |             |                 |
|   | 3              | 162.6         | 89.4        | 883.1       | 1622            |
|   | 4              |               |             |             |                 |
|   | 5              | 216.2         | 126.4       | 392.6       | 97              |
|   | 6              | 181.3         | 92.8        | 760.8       | 686             |
|   | 7              | 225.9         | 147.4       | 281.7       | 3               |
|   | 8              | 191.0         | 104.6       | 847.7       | 231             |

| <b>Variable</b>             | <b>Cluster</b> | <b>Median</b> | <b>Min.</b> | <b>Max.</b> | <b><i>n</i></b> |
|-----------------------------|----------------|---------------|-------------|-------------|-----------------|
| Surface                     | 1              | 1.68          | 0.00        | 89.00       | 376             |
| Si(OH) <sub>4</sub><br>(μM) | 2              | 4.75          | 0.00        | 55.16       | 52              |
|                             | 3              | 0.26          | 0.00        | 17.90       | 1611            |
|                             | 4              | 6.63          | 0.30        | 88.53       | 134             |
|                             | 5              | 1.88          | 0.00        | 127.11      | 525             |
|                             | 6              | 0.68          | 0.00        | 18.95       | 778             |
|                             | 7              | 2.17          | 0.00        | 37.36       | 293             |
|                             | 8              | 1.22          | 0.00        | 20.75       | 321             |
|                             | Bottom         | 1             | 0.99        | 0.00        | 3.93            |
| Si(OH) <sub>4</sub><br>(μM) | 2              |               |             |             |                 |
|                             | 3              | 0.31          | 0.00        | 17.89       | 1514            |
|                             | 4              |               |             |             |                 |
|                             | 5              | 1.67          | 0.00        | 30.20       | 91              |
|                             | 6              | 0.77          | 0.00        | 18.35       | 643             |
|                             | 7              | 0.32          | 0.30        | 0.34        | 2               |
|                             | 8              | 1.21          | 0.00        | 6.65        | 214             |
|                             | Surface        | 1             | 1.30        | 0.00        | 37.00           |
| Turbidity<br>(NTU)          | 2              | 1.20          | 0.20        | 5.55        | 56              |
|                             | 3              | 0.31          | 0.00        | 9.30        | 1706            |
|                             | 4              | 0.77          | 0.00        | 7.70        | 143             |
|                             | 5              | 0.87          | 0.00        | 16.20       | 561             |
|                             | 6              | 0.55          | 0.00        | 8.80        | 832             |
|                             | 7              | 0.95          | 0.00        | 17.35       | 315             |
|                             | 8              | 1.35          | 0.00        | 11.84       | 337             |
|                             | Bottom         | 1             | 1.66        | 0.00        | 9.10            |
| Turbidity<br>(NTU)          | 2              | 1.11          | 1.01        | 1.21        | 2               |
|                             | 3              | 0.36          | 0.00        | 11.18       | 1603            |
|                             | 4              | 1.04          | 1.01        | 2.60        | 5               |
|                             | 5              | 0.80          | 0.00        | 16.90       | 116             |
|                             | 6              | 0.59          | 0.00        | 7.95        | 696             |
|                             | 7              | 0.72          | 0.00        | 4.89        | 12              |
|                             | 8              | 1.55          | 0.00        | 15.96       | 227             |
|                             | Surface        | 1             | 36.2        | 28.8        | 39.6            |
| Salinity                    | 2              | 36.2          | 29.6        | 40.3        | 56              |
|                             | 3              | 36.2          | 26.7        | 37.8        | 1709            |
|                             | 4              | 36.1          | 27.7        | 40.9        | 143             |
|                             | 5              | 36.3          | 29.5        | 40.0        | 543             |
|                             | 6              | 36.2          | 29.5        | 38.5        | 811             |
|                             | 7              | 36.3          | 28.0        | 40.4        | 310             |
|                             | 8              | 36.2          | 30.4        | 38.5        | 339             |

| <b>Variable</b>                | <b>Cluster</b> | <b>Median</b> | <b>Min.</b> | <b>Max.</b> | <b><i>n</i></b> |
|--------------------------------|----------------|---------------|-------------|-------------|-----------------|
| Bottom<br>Salinity             | 1              | 36.1          | 28.8        | 39.7        | 404             |
|                                | 2              | 36.2          | 29.6        | 40.2        | 55              |
|                                | 3              | 36.2          | 32.6        | 37.8        | 1698            |
|                                | 4              | 36.0          | 27.7        | 40.9        | 143             |
|                                | 5              | 36.3          | 29.5        | 40.0        | 539             |
|                                | 6              | 36.3          | 30.5        | 38.5        | 803             |
|                                | 7              | 36.3          | 28.0        | 40.4        | 307             |
|                                | 8              | 36.2          | 30.4        | 38.5        | 338             |
| Surface<br>Temperature<br>(°C) | 1              | 27.7          | 17.8        | 36.1        | 405             |
|                                | 2              | 27.9          | 21.2        | 32.1        | 56              |
|                                | 3              | 26.5          | 16.3        | 32.2        | 1710            |
|                                | 4              | 28.1          | 20.9        | 34.6        | 143             |
|                                | 5              | 27.8          | 15.1        | 39.6        | 544             |
|                                | 6              | 27.5          | 15.4        | 33.0        | 814             |
|                                | 7              | 28.0          | 18.4        | 35.0        | 310             |
|                                | 8              | 26.1          | 18.4        | 34.5        | 340             |
| Bottom<br>Temperature<br>(°C)  | 1              | 27.7          | 17.6        | 33.4        | 404             |
|                                | 2              | 27.8          | 21.2        | 32.1        | 55              |
|                                | 3              | 25.9          | 16.3        | 32.0        | 1699            |
|                                | 4              | 28.1          | 20.3        | 32.7        | 143             |
|                                | 5              | 27.8          | 15.1        | 33.4        | 542             |
|                                | 6              | 27.0          | 15.4        | 32.6        | 805             |
|                                | 7              | 28.0          | 18.4        | 36.8        | 307             |
|                                | 8              | 25.9          | 17.7        | 34.5        | 339             |
| $K_d$<br>( $m^{-1}$ )          | 1              | 0.333         | 0.004       | 2.562       | 309             |
|                                | 2              | 0.311         | 0.021       | 1.856       | 34              |
|                                | 3              | 0.148         | 0.004       | 2.747       | 1245            |
|                                | 4              | 0.404         | 0.090       | 3.274       | 69              |
|                                | 5              | 0.342         | 0.005       | 3.137       | 344             |
|                                | 6              | 0.224         | 0.003       | 3.410       | 582             |
|                                | 7              | 0.372         | 0.011       | 2.983       | 215             |
|                                | 8              | 0.288         | 0.011       | 2.056       | 252             |
| Surface<br>$DO_{sat}$<br>(%)   | 1              | 93.0          | 43.1        | 165.5       | 405             |
|                                | 2              | 89.8          | 65.4        | 118.9       | 56              |
|                                | 3              | 89.3          | 43.4        | 191.6       | 1687            |
|                                | 4              | 93.0          | 65.3        | 148.2       | 143             |
|                                | 5              | 90.6          | 42.9        | 153.3       | 538             |
|                                | 6              | 88.8          | 38.1        | 158.5       | 808             |
|                                | 7              | 90.1          | 38.6        | 130.9       | 310             |
|                                | 8              | 92.0          | 31.2        | 169.9       | 339             |

| <b>Variable</b>                    | <b>Cluster</b> | <b>Median</b> | <b>Min.</b> | <b>Max.</b> | <b><i>n</i></b> |
|------------------------------------|----------------|---------------|-------------|-------------|-----------------|
| Bottom<br>DO <sub>sat</sub><br>(%) | 1              | 93.3          | 41.6        | 166.9       | 404             |
|                                    | 2              | 90.1          | 65.4        | 125.1       | 55              |
|                                    | 3              | 89.0          | 19.3        | 207.0       | 1660            |
|                                    | 4              | 93.4          | 65.2        | 149.6       | 143             |
|                                    | 5              | 91.3          | 42.9        | 152.2       | 538             |
|                                    | 6              | 89.0          | 46.7        | 144.0       | 796             |
|                                    | 7              | 90.1          | 32.4        | 132.0       | 307             |
|                                    | 8              | 91.9          | 41.2        | 171.4       | 337             |
| $\Delta\sigma_\tau$                | 1              | 0.000         | -0.743      | 6.528       | 403             |
|                                    | 2              | 0.000         | -0.222      | 0.371       | 55              |
|                                    | 3              | 0.042         | -3.185      | 6.640       | 1688            |
|                                    | 4              | 0.000         | -0.370      | 1.344       | 143             |
|                                    | 5              | 0.000         | -1.440      | 4.762       | 535             |
|                                    | 6              | 0.033         | -1.512      | 4.439       | 799             |
|                                    | 7              | 0.000         | -4.424      | 4.355       | 307             |
|                                    | 8              | 0.000         | -0.743      | 3.737       | 339             |